

Response to Anonymous Referee #1:

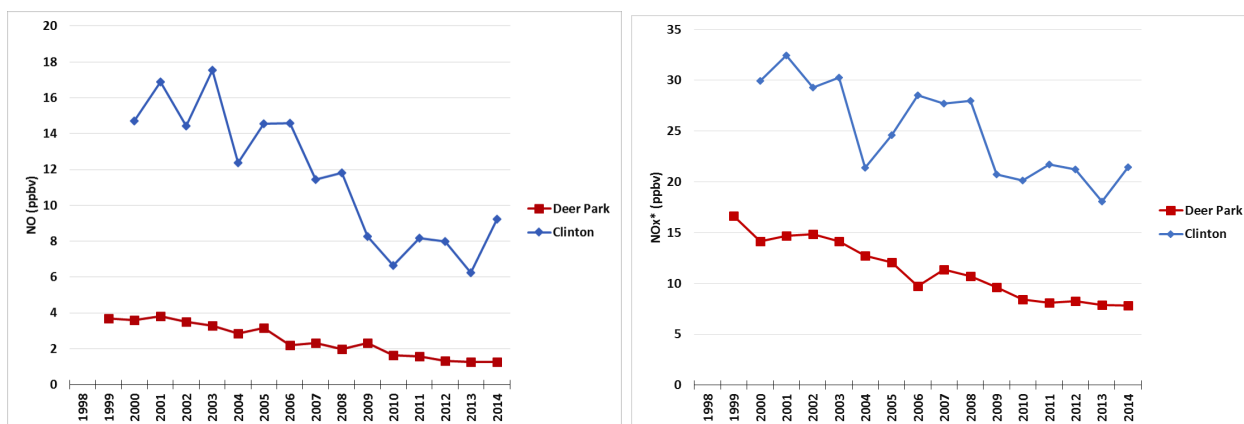
We thank the reviewer for providing insightful comments and helpful suggestions that have substantially improved the manuscript. Below we have included the review comments followed by our responses in italic. In the revision of this manuscript, we have highlighted those changes accordingly in blue font.

- 1) Review of “Ozone production and its sensitivity to NO_x and VOCs: results from the DISCOVER-AQ field experiment, Houston 2013” The authors state several times that these results have important emissions control policy implications but it is not clear what type of program implementation would be needed based on the diurnal ozone production efficiencies presented here.

Response: We are not suggesting a specific implementation program (which is beyond the scope of this work), however, are suggesting that it may be more beneficial at certain locations, during certain times of day, to regulate VOCs based on the diurnal ozone production efficiencies we report. We are providing a scientific basis through which policy makers could develop an emission reduction strategy.

- 2) Given that this paper is focused on NO_x and VOC contribution to O_3 production the authors should provide NO_x and VOC measurements from this study and also compare those with previous Houston field studies to provide more context about how these pollutants are decreasing and for VOC how total VOC and VOC reactivity is decreasing to support conclusions about ozone production efficiency. Also, a comparison with another area like Baltimore would be useful.

Response: Both NO_x and VOC levels in Houston have been continuously decreasing in the past 15-20 years as shown in Figure 1(S1 in paper), the time series of NO, NO_x , ethene, and propene at two monitoring sites near the Houston Ship Channel.



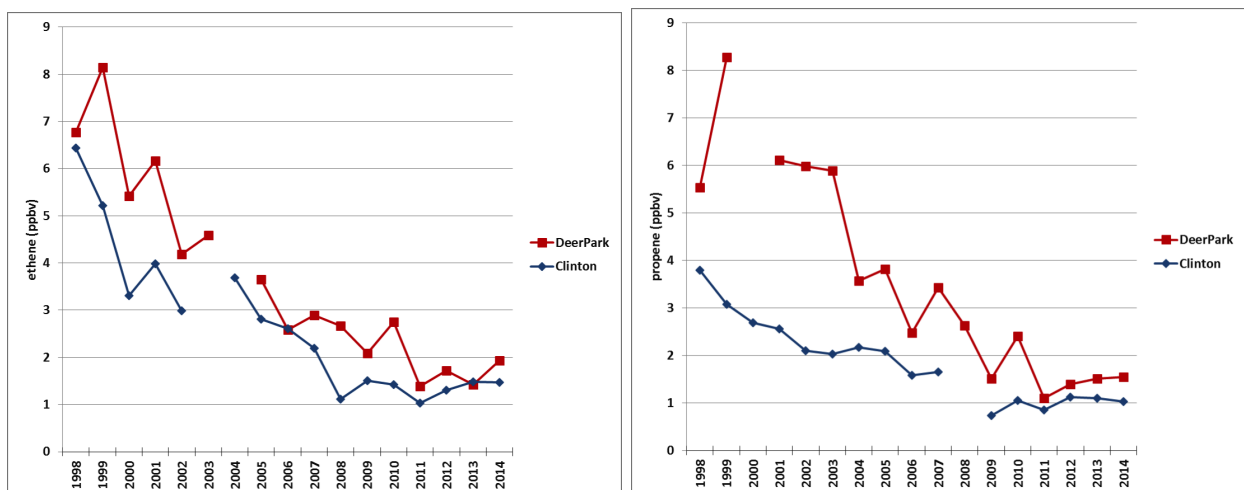


Figure 1. Time series of NO, NO_x, ethene and propene concentrations at the Deer Park and Clinton sites from 1998 to 2014. The Deer Park site is located southeast of the Ship Channel. The Clinton site is located on the northwestern end of the Ship Channel. Each data point represents an average of hourly samples collected between July 1 and November 30 for each year. Missing data points indicate that too few valid samples (< 70%) were collected during that year. NO and NO_x* data collected hourly using chemiluminescence sampler with molybdenum catalyst to convert NO_x* (not true NO_x because Mo catalyst converts other N species besides NO₂ to NO) to NO. VOC data collected over a 40-minute period each hour using automated gas chromatography with cryogenic pre-concentration.

The NO_x levels and OH reactivity in Houston during DAQ2013 and in Maryland during DAQ2011 are quite different, as shown in Figure 2. Houston has much higher NO_x levels throughout the day. For OH reactivity, it is greater in Houston than in Maryland in the morning, but is comparable in both locations in the afternoon. Note as shown in Figure 4, due to different emission sources, in Houston anthropogenic VOCs are the main contributor to the OH reactivity from VOCs, while in Maryland, biogenic VOCs (mainly isoprene) dominates the OH reactivity from VOCs. Different NO_x levels and different VOC sources in Houston and Maryland are responsible for the different OPE values in the two areas.

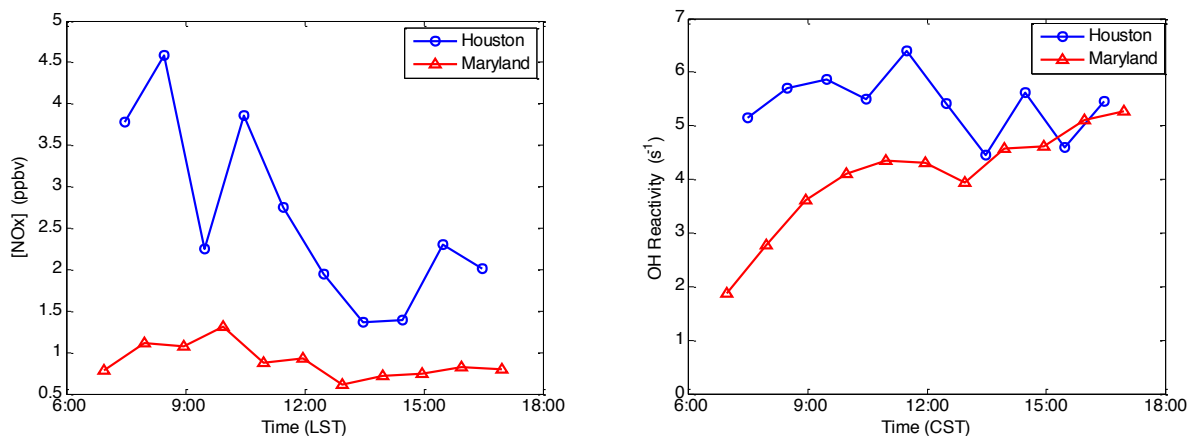


Figure 2. Diurnal variations of NO_x (left) and OH reactivity (right) in Houston (linked blue circles) during DAQ2013 and in Maryland (linked red triangles) during DAQ2011.

- 3) The authors provide CMAQ simulated ozone production efficiency but provide no information about the emission inventory used for the simulation and how well the model predicted NO_x, NO_z, VOC, and O₃ compared with the aircraft and surface measurements made during the field study. Is it ok that the model predicts a similar OPE to the box model but not capture the magnitudes of the precursors or ozone correctly? The information presented about OPE is useful, but additional work is needed for this to provide a more comprehensive understanding of ozone production in Houston with respect to the models used by regulators for decision support and context from the many previous Houston field studies.

Response: The WRF and CMAQ model options are described in Table 1. In Section 2.3, we also added the following a few sentences to describe the emissions we used in the CMAQ simulations: “The 2012 baseline anthropogenic emissions from the Texas Commission on Environmental Quality (TCEQ) were used as input to CMAQ. These emissions contain the most-up-to-date Texas anthropogenic emissions inventory and a compilation of emissions estimates from Regional Planning Offices throughout the US. Biogenic emissions were calculated online within CMAQ with Biogenic Emission Inventory System (BEIS). Lightning emissions were also calculated online within CMAQ.”

CMAQ simulated a high bias in surface and aloft ozone (Tables 1). CMAQ also simulated a low bias in CO, CH₂O, isoprene, NO₂, and NO aloft and a high bias in NO_y aloft (Table 2). Recent work has shown that oceanic emissions of iodine and bromine result in ozone destruction (Carpenter et al., 2013). The high ozone bias in our results is expected due to the lack of oceanic iodine and bromine emissions and the associated chemistry. Biases in surface ozone are larger near the coastline (i.e., Galveston) than sites inland (i.e., Conroe).

Table 1. Mean bias (MB), normalized mean bias (NMB), normalized mean error (NME), root mean square error (RMSE), and Gross Error (GE) of surface ozone for the 2nd iterative 1 km WRF simulations covering all of September 2013.

	Surface Ozone (ppbv)
MB	9.5
NMB (%)	39
NME (%)	51
RMSE	15
GE	12

Table 2. Second iterative 1 km CMAQ simulated mean bias (MB), normalized mean bias (NMB), normalized mean error (NME), and root mean square error (RMSE) of O₃, CO, CH₂O, Isoprene (ISO), NO₂, NO, and NO_y covering measurements made onboard the NASA P-3B aircraft on all flight days during the DISCOVER-AQ field campaign.

		O ₃	CO	CH ₂ O	ISO	NO ₂	NO	NO _y
Model	MB	0.8	-5.8	-0.3	-0.02	-0.5	-0.3	0.04
	NMB	1.4	-4.8	-16	-7.7	-39	-66	1.3
	NME	15	17	37	70	70	84	61
	RMSE	12	35	1.4	0.7	3.1	2.2	4.7

- 4) The last half of the introduction section reads like a white paper on the Houston DISCOVER-AQ field study. Since this paper does not present any information relevant to the mission of that field study which was to validate satellite measurements the discussion of the DISCOVER-AQ campaign could be de-emphasized in favor of more time spent on the multitude of historical field studies in the Houston area. Also, the authors never clearly state in the introduction what they are presenting and why that information is novel.

Response: We have removed lines 89-96 and combine lines 97 – 100 and took out lines 102-106. We edited lines 81-84 to read: “In the work presented here, we provide investigations of spatial and temporal variations of ozone production and its sensitivity to NO_x and VOCs to provide a scientific basis to develop a non-uniform emission reduction strategy for O₃ pollution control in urban areas such as Houston.”

- 5) The authors do not need to explain why CB05 is used rather than CBIV, but an explanation about why CB05 was used rather than the newer version CB6 is necessary. At several points in the manuscript the authors note that organic nitrate fate can confound OPE interpretation so the choice of an older Carbon Bond mechanism that has a less realistic treatment of organic nitrates is needed. Also, it is not clear why all species have the same two-day deposition lifetime. Species like O₃ and HNO₃ deposit out of the atmosphere and very different rates.

Response: CB05 is the most up to date Carbon Bond mechanism in CMAQ (i.e., CB6 has not been implemented into CMAQ at the time the analysis was performed). The box model was constrained for all long-lived measured species like ozone and HNO₃ and we do not assume a two-day deposition lifetime. An additional two-day lifetime due to deposition and heterogeneous losses is assumed for calculated species in the box model. Most calculated species like OH, HO₂ and RO₂ are reactive intermediates and have lifetimes on the order of seconds to minutes, much shorter than 2 days. Adding this additional two-day lifetime would not affect the model results at all. There are a few long-lived species (like organic acid and alcohols) calculated in the model that could potentially accumulate to levels much higher than the levels in the ambient air. We have revised this sentence: “An additional lifetime of two days was assumed for some calculated long lived species such as organic acids and alcohols to avoid unexpected accumulation of these species in the model.”

- 6) Please provide information about the emission inventory and modeling used as input to the CMAQ simulation and the source of the initial and boundary conditions.

Response: The WRF and CMAQ model options have been described in Table 1. In Section 2.3, we also added the following a few sentences for the emissions we used in the CMAQ simulations: “The 2012 baseline anthropogenic emissions from the Texas Commission on Environmental Quality (TCEQ) were used as input to CMAQ. These emissions contain the most-up-to-date Texas anthropogenic emissions inventory and a compilation of emissions estimates from Regional Planning Offices throughout the US Biogenic emissions was calculated online within CMAQ with Biogenic Emission Inventory System (BEIS). Lightning emissions were also calculated online within CMAQ.” It is also listed in Table 1 of this manuscript.

- 7) In the results section, please provide some comparison of CMAQ estimated VOC, speciated VOC, NO, NO₂, HNO₃, PANs, HNO₃, and O₃ with measurements.

Response: An evaluation of the improved WRF and CMAQ model simulations for the entire month of September 2013 was conducted. Statistics used to evaluate WRF and CMAQ are described Tables 3. CMAQ simulated a high bias in surface and aloft ozone (Table 1). CMAQ also simulated a low bias in CO, CH₂O, isoprene, NO₂, and NO aloft and a high bias in NO_y aloft (Table 2). Recent work has shown that oceanic emissions of iodine and bromine result in ozone destruction. The high ozone bias in our results is expected due to the lack of oceanic iodine and bromine emissions and the associated chemistry. Biases in surface ozone are larger near the coastline (i.e., Galveston) than sites inland (i.e., Conroe) as shown in Figure 3.

Table 3. Definition of the statistics used in WRF and CMAQ model evaluations. In these equations M represents the model results, O represents the observations, and N is the number of data points.

Mean Bias (MB)	$MB = \frac{1}{N} \sum_{i=1}^N (M_i - O_i)$
Normalized Mean Bias (NMB)	$NMB = \frac{\sum_{i=1}^N (M_i - O_i)}{\sum_{i=1}^N O_i} \times 100\%$
Normalized Mean Error (NME)	$NME = \frac{\sum_{i=1}^N M_i - O_i }{\sum_{i=1}^N O_i} \times 100\%$
Root Mean-Square Error (RMSE)	$RMSE = \sqrt{\frac{1}{N} \sum_{i=1}^N (M_i - O_i)^2}$
Gross Error (G)	$GE = \frac{1}{N} \sum_{i=1}^N M_i - O_i $

Table 4. Mean bias (MB), normalized mean bias (NMB), normalized mean error (NME), root mean square error (RMSE), and Gross Error (GE) of 2 m temperature, 10 m wind speed, and 10 m wind direction for the 2nd iterative 1 km WRF simulations covering all of September 2013.

	2 m Temperature (K)	10 m Wind Speed (m/s)	10 m Wind Direction (deg)
	Model	Model	Model
MB	0.2	-0.8	32
NMB (%)	0.1	-17	26
NME (%)	0.4	36	26
RMSE	1.6	2.3	51
GE	1.2	1.7	32

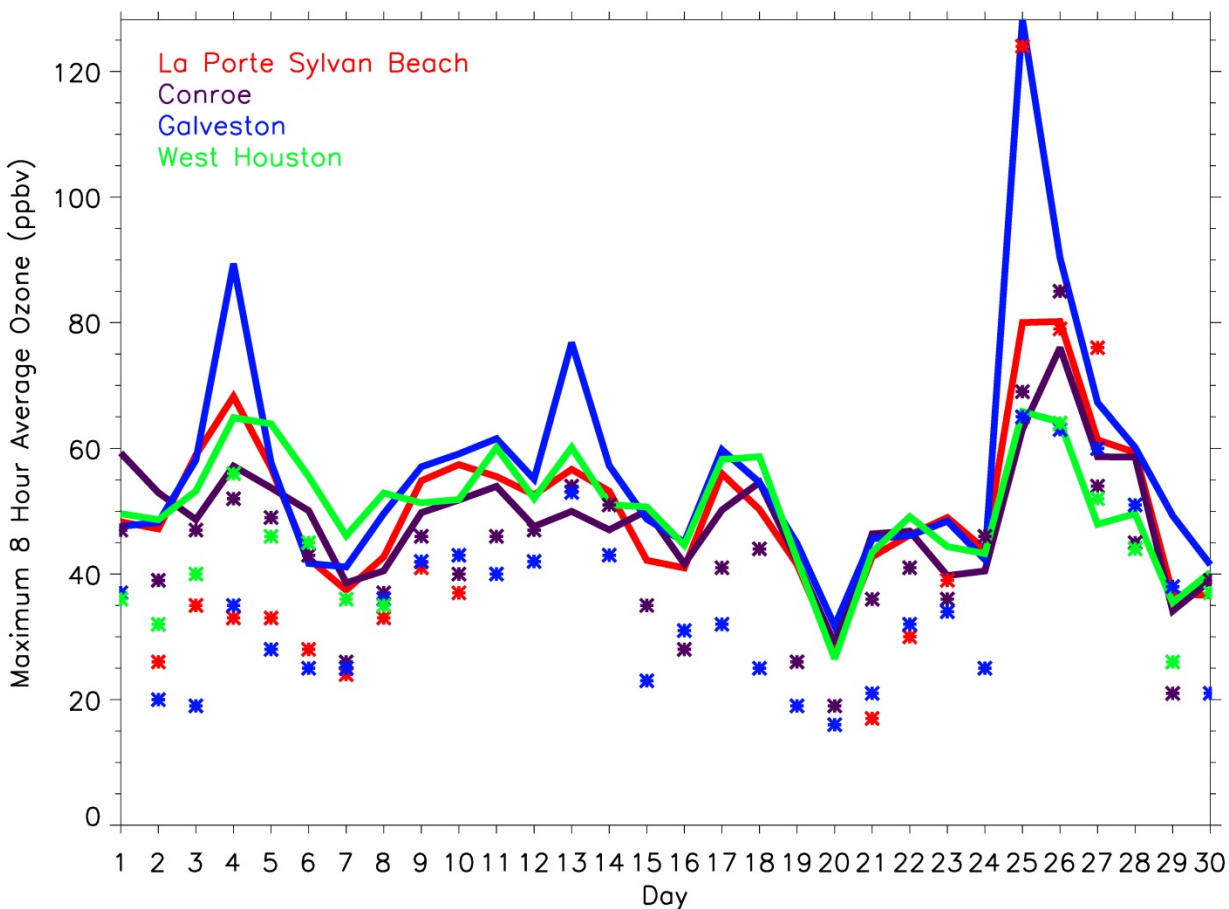


Figure 3. Observed (*) and CMAQ simulated (solid lines) maximum 8 hour average ozone at La Porte Sylvan Beach (red), Conroe (purple), Galveston (blue), and West Houston (green) during September 2013.

- 8) The authors suggest one difference in OPE between Houston and Baltimore is due to reactivity. Please provide speciated VOC concentrations from each field study by reactivity so this relationship is clearer.

Response: The median OH reactivity due to non-methane hydrocarbons (NMHCs) was 3.3 s^{-1} observed during DISCOVER-AQ 2013 in Houston and 1.2 s^{-1} observed during DISCOVER-AQ 2011 in Maryland. As shown in Figure 4, alkanes and alkenes were dominant contributors to the OH reactivity due to NMHCs in Houston in 2013, while isoprene and alkanes were dominant contributors to the OH reactivity due to NMHCs in Maryland in 2011. The differences in overall OH reactivity and its distributions in the two locations are responsible to the different OPEs in the two different environments. We have included this in the Supporting Information.

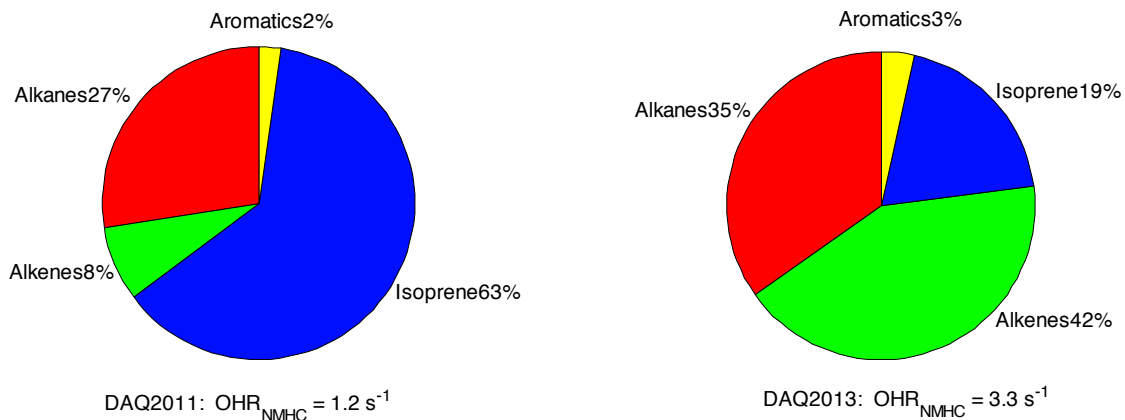


Figure 4. Distributions of OH reactivity due to non-methane hydrocarbons in DISCOVER-AQ 2011 in Maryland (left) and 2013 in Houston (right).

- 9) The authors make a lot of strong conclusions about trends in OPE when NO_x is greater or less than 1 ppb as shown in Figure 14. The points in Figure 14 do not show a distinct relationship above or below any level of the NO_x concentrations. Perhaps box plots binned by NO_x concentration would be a better way to show this type of relationship (if it really exists).

Response: We have updated Figure 13 by adding median OPE values binned by NO_x concentration on top of the individual data points and the trend seems more distinct.

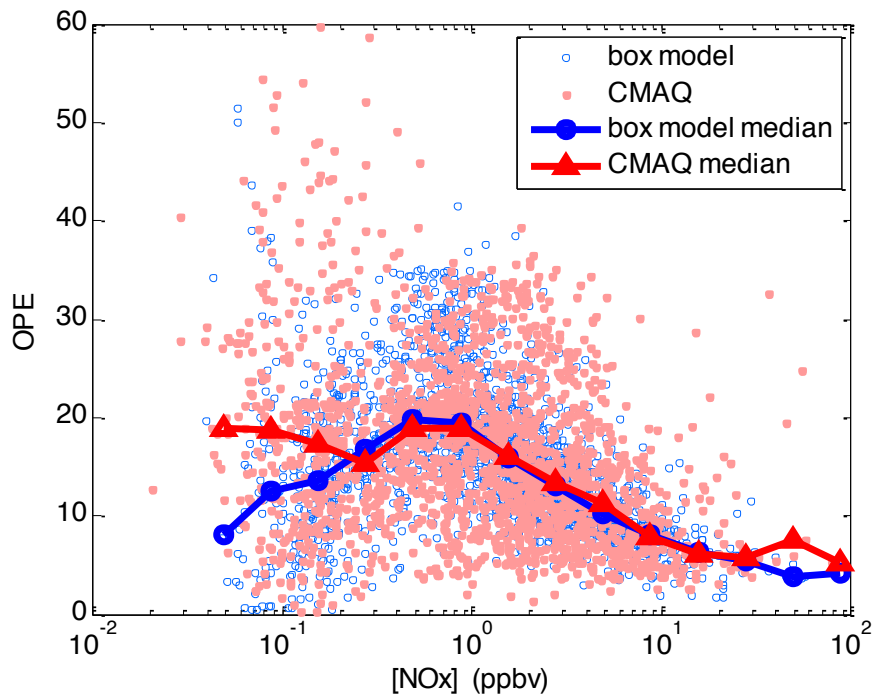


Figure 13. Ozone production efficiency (OPE) versus NO_x in the box model (blue circles) and the CMAQ model (pink dots) results. The linked blue circles show the median OPE values binned by NO_x concentration in the box model, while the linked red triangles show the median OPE values binned by NO_x concentration in the CMAQ model, OPE is calculated according to its definition as the net ozone formation rate divided by the formation rate of NO_z.

Response to Anonymous Referee #2:

We thank the reviewer for providing insightful comments and helpful suggestions that have substantially improved the manuscript. Below we have included the review comments followed by our responses in italic. In the revision of this manuscript, we have highlighted those changes accordingly in blue font.

1. The analyses performed and the approach used are tried and true so technically, there are no major faults with the work (though I question the use of a box model in Houston when the meteorology is so complex - why not just use the 3D model as it can provide answers to some of the questions asked and the ambient data can be used for model evaluation). However, due to a lack of novelty and a lack of truly new findings that warrant an entire manuscript, I am unable to recommend this manuscript for publication in ACP.

Response: The reviewer's comment prompted us to re-examine the literature, where we found a few more relevant papers (i.e. Thielmann et al., 2002; Zaveri et al., 2003; Ryerson et al., 2003; Griffin et al., 2003, Kommalapati et al., 2016), but none that thoroughly addressed the issues that we cover in this paper.

In response to why we did not just use a 3D model, the box model is constrained to observed meteorological parameters and chemical species such as O₃, NO_x, CO, and some VOCs, which we find to be more useful than a 3D model for this kind of analysis since it eliminates some uncertainties, or errors that a 3D model could have. A 3D CTM may have major problems with the emissions inventories as described by Yu et al. (2012) and Travis et al. (in review in ACPD, 2016), who show that modeled NO_y was twice as high than observed. Our box model simulation could reduce uncertainties in the ozone production and sensitivity calculations.

We have stated at the end of Section 2.2: "The box model analysis is necessary for ozone production and its sensitivity to NO_x and VOCs because the box model was constrained to measured species (e.g., NO, NO₂, CO, HCHO, etc.) and meteorological parameters (e.g., photolysis frequencies) that are essential to calculate ozone production rates. Even though there is good agreement in general between the box model and the 3D model, there are still some differences between the measurements and the output from the 3D model, e.g., NO_x, CO, HCHO and photolysis frequencies."

2. With regard to figures, Figure 1 is not necessary (the ozone isopleth is "classic"), Figure 2 would be better as a map with points/labels as the extraneous stuff is distracting, and Figures 3 and 4 can be combined. In addition, some of the figures are intuitive based on previous work in Houston and other locations (5, 6, 8, and 9).

Response: We would like to keep Figure 1 in the paper. Since Figure 1 is ozone production and not ozone concentration as traditional EKMA O₃ isopleth diagrams are, it could provide useful information for the reader about how ozone production changes with regarding to NO_x and VOC and NO_x and VOC sensitive regimes of ozone production. As suggested, we have changed

Figure 2 to a map with points and labels. Figures 3 and 4 are combined. Figures 5, 6, 8 and 9 are the results from the DISCOVER-AQ Houston campaign showing spatial and temporal variations of ozone production and its sensitivity to NO_x and VOCs. To our knowledge, there has not been a single study that covers such a large spatial range on this topic, and the data from this campaign provide us the unique opportunity to do such an analysis.

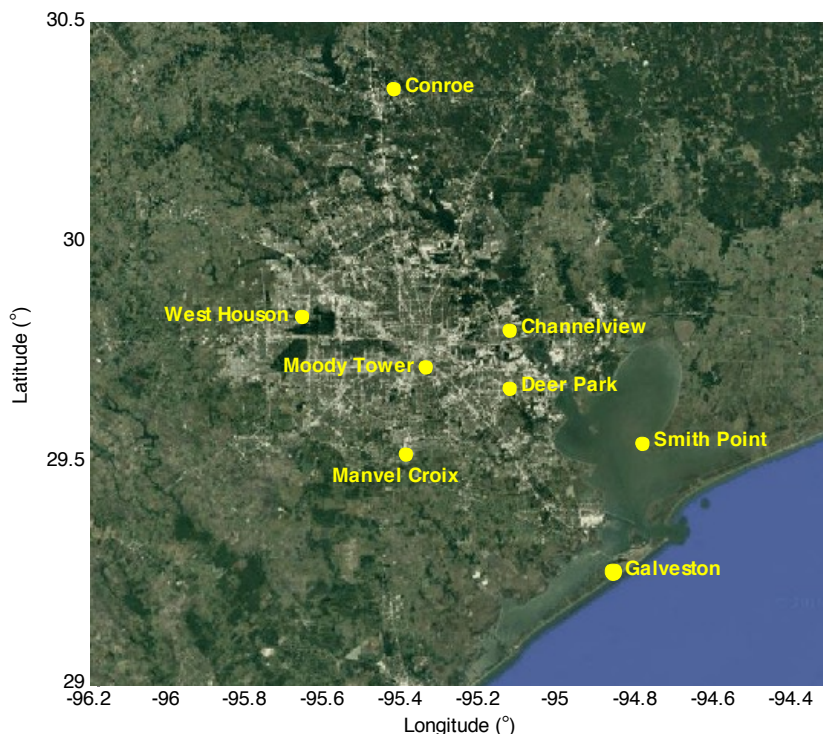


Figure 2. DISCOVER-AQ ground and spiral sites (yellow dots) during the September 2013 Houston campaign.

3. My largest criticism of this work is that it is known from three previous field campaigns that ozone production rates and sensitivities in Houston are temporally and spatially dependent. It seems to be that the most new information appears on lines 203-205 (line 206 is intuitive) regarding O₃ loss and the split between RO₂ and HO₂ reactions with NO (unless this information is published elsewhere and I am unaware) and on line 255+ where it is noted that OPE has decreased in Houston compared to previous campaigns (due to the decrease in NO_x emissions). I do not believe that these warrant a manuscript by themselves.

Response: The reviewer was right that there have been some previous studies, including three previous studies in Houston in 2000, 2006, and 2009 and some others in other locations, on ozone production and its relationships to NO_x and VOCs (e.g., Kleinman et al., 2002; Ryerson et al., 2003; Newman et al., 2009; Mao et al., 2010; Chen et al., 2010; Ren et al., 2013), but to our

knowledge, none of them has done systematic analysis on ozone production and its sensitivity to NO_x and VOCs and covers such large spatial (urban and suburban) and temporal ranges as the DISCOVER-AQ Houston campaign does in 2013. For example, the SHARP study in 2009 (Ren et al., 2013) and the Texas Air Quality Study Radical and Aerosol Measurement Project (TRAMP) in 2006 (Mao et al., 2010; Chen et al., 2010) did cover ozone production and its sensitivity to NO_x and VOCs, but they were focus on the data collected at a single location at Moody Tower at the University of Houston. Kleinman et al. (2002) and Ryerson et al., (2003) from TexAQS I in 2000 and Newman et al. (2009) from TexAQS II in 2006 discussed ozone production efficiencies (OPE), but they did not talk about the dependence of OPE on NO_x and did not cover the sensitivity of ozone production to NO_x and VOCs. The rich data set collected during the DISCOVER-AQ Houston campaign provides us a unique opportunity to perform this systematic analysis and we believe it is worth to inform the atmospheric chemistry community about the latest findings from this study to reflect the changes in chemical conditions (e.g., emissions) in Houston since previous studies.

4. The authors do not put Houston in the context of other locations. For example, they state on line 68 that "there are a limited number of observation-based studies on ozone production and its sensitivity to NO_x and VOCs." There have been such studies made in Houston (SHARP, TEXAQS I and II) as well as in other locations across the US (Nashville, New England) and Europe. It would be appropriate to make such comparisons.

Response: We have cited results from other studies in other locations (e.g., Zaveri et al., 2003; Griffin et al., 2004; Thielmann et al., 2002) in the introduction and compared the results from this study to those from other locations. Our study is unique in that it examines the spatial and temporal variations in ozone production and its sensitivity. Other studies are mostly ground-based (i.e., single location like SHARP) or with limited spatial/temporal coverage. We found a higher OPE in this study than what was found in previous studies in Houston, which is probably due to continuous emission control as NO_x levels were continuously pushed to ~1ppbv and thus we got a higher OPE.

We have revised this sentence as: "There are some observation-based studies on ozone production and its relationships with NO_x and VOCs [e.g., Thielmann et al., 2002; Zaveri et al., 2003; Ryerson et al., 2003; Griffin et al., 2003; Kleinman et al., 2005a; Neuman et al., 2009; Mao et al., 2010; Ren et al., 2013]"

In Section 3.1, we have added one sentence: "Similar instantaneous ozone production rates have been observed in two previous studies in Houston in 2000 and 2006 [Kleinman et al., 2002a; Mao et al., 2010]."

In Section 3.2, we revised a sentence to: "Houston area OPE values range from about a factor of 1.3 to 2 higher than the OPEs calculated from the DISCOVER-AQ 2011 study in Maryland, likely due to higher photochemical reactivity in Houston (Figure S4). The 2011 Maryland OPEs

ranged from 3.4 to 6.1 when all measured data below 1 km are used (Ren, X., unpublished data). An OPE of ~8 was calculated [He et al., 2013] for the 2011 Maryland DISCOVER-AQ campaign for measured data below the 850 hPa level during vertical spirals with a strong linear correlation ($r^2 > 0.8$) between O_x and NO_2 . Additionally, OPEs of 7.7-9.7 were obtained from a ground site during the New England Air Quality Study (NEAQS) 2002 (Griffin et al., 2004).”

5. What is the basis for assuming a two-day lifetime for all calculated species to avoid build up?

Response: We do not provide a citation because we chose this value somewhat arbitrarily. By decreasing or increasing two days to one or ten days, it would not have much affect on the simulation results. This is because the box model already constrained all measured long-lived measured species. The additional lifetime of two days for the calculated species is to account for losses due to dry and wet deposition, vertical and horizontal diffusion, and to prevent accumulation of long-lived species in the box model. Most calculated species like OH, HO₂ and RO₂ are reactive intermediates and have lifetimes on the order of seconds to minutes, much shorter than 2 days. By adding this additional two-day lifetime would not affect the model results at all. There are a few long-lived species (like organic acid and alcohols) calculated in the model that could potentially accumulate to levels much higher than the levels in the ambient air.

We have revised this sentence: “An additional lifetime of two days was assumed for some calculated long lived species such as organic acids and alcohols to avoid unexpected accumulation of these species in the model.”

Additional References

Carpenter, L. J., S. M. MacDonald, M. D. Shaw, R. Kumar, R. W. Saunders, R. Parthipan, J. Wilson, and J. M. C. Plane (2013), Atmospheric iodine levels influenced by sea surface emissions of inorganic iodine, Nat Geosci, 6(2), 108-111.

Griffin, R. J., C. A. Johnson, R. W. Talbot, H. Mao, R. S. Russo, Y. Zhou, and B. C. Sive (2004), Quantification of ozone formation metrics at Thompson Farm during the New England Air Quality Study (NEAQS) 2002, J. Geophys. Res., 109, D24302, doi:10.1029/2004JD005344.

Kommalapati, R. R., Z. Liang, and Z. Huque (2016), Photochemical model simulations of air quality for Houston-Galveston-Brazoria area and analysis of ozone-NO (x) -hydrocarbon sensitivity, International Journal of Environmental Science and Technology, 13(1), 209-220.)

Ryerson, T. B., et al., Effect of petrochemical industrial emissions of reactive alkenes and NOx on tropospheric ozone formation in Houston, Texas, J. Geophys. Res., 108(D8), 4249, doi:10.1029/2002JD003070, 2003.

Thielmann, A., A. S. H. Pre'vo't, and J. Staehelin, Sensitivity of ozone production derived from

field measurements in the Italian Po basin, J. Geophys. Res., 107(D22), 8194, doi:10.1029/2000JD000119, 2002.

Yu, S. C., et al. (2012), Comparative evaluation of the impact of WRF-NMM and WRF-ARW meteorology on CMAQ simulations for O₃ and related species during the 2006 TexAQS/GoMACCS campaign, Atmospheric Pollution Research, 3(2), 149-162.

Zaveri, R. A., C. M. Berkowitz, L. I. Kleinman, S. R. Springston, P. V. Doskey, W. A. Lonneman, and C. W. Spicer, Ozone production efficiency and NO_x depletion in an urban plume: Interpretation of field observations and implications for evaluating O₃-NO_x-VOC sensitivity, J. Geophys. Res., 108(D14), 4436, doi:10.1029/2002JD003144, 2003.

List of changes in revised, *marked up* manuscript below: (line numbers may be slightly off on unmarked up version)

1) We revised the sentences on lines 68-70 to read:

“There are some observation-based studies on ozone production and its relationships with NO_x and VOCs [e.g., Thielmann et al., 2002; Zaveri et al., 2003; Ryerson et al., 2003; Griffin et al., 2003; Kleinman et al., 2005a; Neuman et al., 2009; Mao et al., 2010; Ren et al., 2013]”

2) We have removed lines 91-98 and combine lines 99 – 102 and took out lines 104-108. We edited lines 83-86 to read:

“In the work presented here, we provide investigations of spatial and temporal variations of ozone production and its sensitivity to NO_x and VOCs to provide a scientific basis to develop a non-uniform emission reduction strategy for O₃ pollution control in urban areas such as Houston.”

3) We have revised the sentence on lines 144-146 to read:

“An additional lifetime of two days was assumed for some calculated long-lived species such as organic acids and alcohols to avoid unexpected accumulation of these species in the model.”

4) We added the following on lines 153-159:

“The box model analysis is necessary for ozone production and its sensitivity to NO_x and VOCs because the box model was constrained to measured species (e.g., NO, NO₂, CO, HCHO, etc.) and meteorological parameters (e.g., photolysis frequencies) that are essential to calculate ozone production rates. Even though there is good agreement in general between the box model and the 3D model, there are still some differences between the measurements and the output from the 3D model, e.g., NO_x, CO, HCHO and photolysis frequencies.”

5) We added the following on lines: 170-176

“The 2012 baseline anthropogenic emissions from the Texas Commission on Environmental Quality (TCEQ) were used as input to CMAQ. These emissions contain the most-up-to-date Texas anthropogenic emissions inventory and a compilation of emissions estimates from Regional Planning Offices throughout the US. Biogenic emissions were calculated online within CMAQ with Biogenic Emission Inventory System (BEIS). Lightning emissions were also calculated online within CMAQ.”

6) On lines 189-190 in Section 3.1, we have added one sentence:

“Similar instantaneous ozone production rates have been observed in two previous studies in Houston in 2000 and 2006 [Kleinman et al., 2002a; Mao et al., 2010].”

7) On lines 257-264 in Section 3.2, we revised a sentence to read:

“Houston area OPE values range from about a factor of 1.3 to 2 higher than the OPEs calculated from the DISCOVER-AQ 2011 study in Maryland, likely due to higher photochemical reactivity in Houston (Figure S4). The 2011 Maryland OPEs ranged from 3.4 to 6.1 when all measured data below 1 km are used (Ren, X., unpublished data). An OPE of ~8 was calculated [He et al., 2013] for the 2011 Maryland DISCOVER-AQ campaign for measured data below the 850 hPa level during vertical spirals with a strong linear correlation ($r^2 > 0.8$) between O_x and NO_z . Additionally, OPEs of 7.7-9.7 were obtained from a ground site during the New England Air Quality Study (NEAQS) 2002 (Griffin et al., 2004).”

8) We updated figure 2 (line 466)

9) We combined originally separate figures into Figure 3 (line 471)

10) We updated figure 8 (line 494)

11) We have updated Figure 13 by adding median OPE values binned by NO_x concentration on top of the individual data points and the trend seems more distinct (line 530)

1 **Ozone Production and Its Sensitivity to NO_x and VOCs: Results from the DISCOVER-AQ**
2 **Field Experiment, Houston 2013**

3 Gina M. Mazzuca¹, Xinrong Ren^{1,2,*}, Christopher P. Loughner^{2,3}, Mark Estes⁵, James H.
4 Crawford⁶, Kenneth E. Pickering^{1,4}, Andrew J. Weinheimer⁷, and Russell R. Dickerson¹

5 ¹Department of Atmospheric and Oceanic Science, University of Maryland, College Park, MD
6 20742, USA

7 ²Air Resources Laboratory, National Oceanic and Atmospheric Administration, College Park,
8 MD 20740, USA

9 ³Earth System Science Interdisciplinary Center, University of Maryland, College Park, MD
10 20740, USA

11 ⁴NASA Goddard Space Flight Center, Greenbelt, MD 20771, USA

12 ⁵Texas Commission on Environmental Quality, Austin, TX 78711, USA

13 ⁶NASA Langley Research Center, Hampton, VA 23681, USA

14 ⁷National Center for Atmospheric Research, Boulder, CO 80307, USA

15

16

17 *Correspondence to: X. Ren (ren@umd.edu)

18

19 **Abstract** An observation-constrained box model based on the Carbon Bond mechanism, Version
20 5 (CB05), was used to study photochemical processes along the NASA P-3B flight track and
21 spirals over eight surface sites during the September 2013 Houston, Texas deployment of the
22 NASA DISCOVER-AQ campaign. Data from this campaign provided an opportunity to examine
23 and improve our understanding of atmospheric photochemical oxidation processes related to the
24 formation of secondary air pollutants such as ozone (O₃). O₃ production and its sensitivity to
25 NO_x and VOCs were calculated at different locations and times of day. Ozone production
26 efficiency (OPE), defined as the ratio of the ozone production rate to the NO_x oxidation rate, was
27 calculated using the observations and the simulation results of the box and Community
28 Multiscale Air Quality (CMAQ) models. Correlations of these results with other parameters,
29 such as radical sources and NO_x mixing ratio, were also evaluated. It was generally found that O₃
30 production tends to be more VOC sensitive in the morning along with high ozone production
31 rates, suggesting that control of VOCs may be an effective way to control O₃ in Houston. In the

32 afternoon, O₃ production was found to be mainly NO_x sensitive with some exceptions. O₃
33 production near major emissions sources such as Deer Park was mostly VOC sensitive for the
34 entire day, other urban areas near Moody Tower and Channelview were VOC sensitive or in the
35 transition regime, and areas farther from downtown Houston such as Smith Point and Conroe
36 were mostly NO_x sensitive for the entire day. It was also found that the control of NO_x emissions
37 has reduced O₃ concentrations over Houston, but has led to larger OPE values. The results from
38 this work strengthen our understanding of O₃ production; they indicate that controlling NO_x
39 emissions will provide air quality benefits over the greater Houston metropolitan area in the long
40 run, but in selected areas controlling VOC emissions will also be beneficial.

41

42 **Keywords** Ozone production; Ozone Production Efficiency; Houston; DISCOVER-AQ

43

44 **1. Introduction**

45 Understanding the non-linear relationship between ozone production and its precursors is
46 critical for the development of an effective ozone (O₃) control strategy. Despite great efforts
47 undertaken in the past decades to address the problem of high ozone concentrations, our
48 understanding of the key precursors that control tropospheric ozone production remains
49 incomplete and uncertain [Molina and Molina, 2004; Xue et al., 2013]. Atmospheric ozone
50 levels are determined by emissions of ozone precursors, atmospheric photochemistry, and
51 transport [Jacob, 1999; Xue et al., 2013]. A major challenge in regulating ozone pollution lies in
52 comprehending its complex and non-linear chemistry with respect to ozone precursors, i.e.,
53 nitrogen oxides (NO_x) and volatile organic compounds (VOCs) that varies with time and location
54 (Figure 1). Understanding the non-linear relationship between ozone production and its
55 precursors is critical for the development of an effective ozone control strategy.

56 Sensitivity of ozone production to NO_x and VOCs represents a major uncertainty for
57 oxidant photochemistry in urban areas [Sillman et al., 1995; 2003]. In urban environments,
58 ozone is formed through photochemical processes when its precursors NO_x and VOCs are
59 emitted into the atmosphere from many sources. Depending on physical and chemical conditions,
60 the production of ozone can be either NO_x-sensitive or VOC-sensitive due to the complexity of
61 these photochemical processes. Therefore, effective ozone control strategies rely heavily on the
62 accurate understanding of how ozone responds to reduction of NO_x and VOC emissions, usually

63 simulated by photochemical air quality models [e.g., Sillman et al., 2003; Lei et al., 2004; Mallet
64 and Sportisse, 2005; Li et al., 2007; Chen et al., 2010; Tang et al., 2010; Xue et al., 2013;
65 Goldberg et al., 2016]. However, those model-based studies have inputs or parameters subject to
66 large uncertainties that can affect not only the simulated levels of ozone but also the ozone
67 dependence on its precursors.

68 There are some observation-based studies of ozone production and its relationships with
69 NO_x and VOCs [e.g., Thielmann et al., 2002; Zaveri et al., 2003; Ryerson et al., 2003; Griffin et
70 al., 2003; Kleinman et al., 2005a; Neuman et al., 2009; Mao et al., 2010; Ren et al., 2013]. Using
71 in-situ aircraft observations, Kleinman et al. [2005a] studied five U.S. cities and found that ozone
72 production rates vary from nearly zero to 155 ppb hr^{-1} with differences depending on precursor
73 concentrations NO_x , and VOCs. They also found that in Houston, NO_x and light olefins are co-
74 emitted from petrochemical facilities leading to the highest ozone production of the five cities
75 [Kleinman et al., 2005a]. Using the data collected at a single surface location during the Study of
76 Houston Atmospheric Radical Precursors (SHARP) in spring 2009, the temporal variation of O_3
77 production was observed: VOC-sensitive in the early morning and NO_x -sensitive for most of the
78 afternoon [Ren et al., 2013]. This is similar to the behavior observed in two previous
79 summertime studies in Houston: the Texas Air Quality Study in 2000 (TexAQS 2000) and the
80 TexAQS II Radical and Aerosol Measurement Project in 2006 (TRAMP 2006) [Mao et al., 2010;
81 Chen et al., 2010]. In a more recent study using measurements in four cities in China, ozone
82 production was found to be in a VOC-sensitive regime in both Shanghai and Guangzhou, but in a
83 mixed regime in Lanzhou [Xue et al., 2013]. In the work presented here, we provide
84 investigations of spatial and temporal variations of ozone production and its sensitivity to NO_x
85 and VOCs to provide a scientific basis to develop a non-uniform emission reduction strategy for
86 O_3 pollution control in urban and suburban areas such as the greater Houston metropolitan area.

87 This work utilized observations made during the Deriving Information on Surface
88 Conditions from COlumn and VERTically Resolved Observations Relevant to Air Quality
89 (DISCOVER-AQ) campaign in Houston in September 2013. This field campaign is unique due
90 to the comprehensive air sampling performed over a large spatial (urban and suburban areas in
91 and around Houston) and temporal (entire month of September 2013) range. Measurements were
92 collected from various platforms including the National Aeronautics and Space Administration
93 (NASA) P-3B and B-200 aircraft, ground surface sites, and mobile laboratories. Eight surface

94 monitoring stations (Smith Point, Galveston, Manvel Croix, Deer Park, Channelview, Conroe,
95 West Houston, and Moody Tower) were selected where the P-3B conducted vertical spirals
96 (Figure 2) [DISCOVER-AQ whitepaper].

97

98 **2. Methods**

99 **2.1 Ozone production Scenarios and Sensitivity**

100 During the day, the photochemical O₃ production rate is essentially the production rate of
101 NO₂ molecules from HO₂ + NO and RO₂ + NO reactions [Finlayson-Pitts and Pitts, 2000]. The
102 net instantaneous photochemical O₃ production rate, P(O₃), can be written approximately as the
103 following equation:

$$104 \quad P(O_3) = k_{HO_2+NO}[HO_2][NO] + \sum k_{RO_{2i}+NO}[RO_{2i}][NO] - k_{OH+NO_2+M}[OH][NO_2][M] - P(RONO_2) \\ - k_{HO_2+O_3}[HO_2][O_3] - k_{OH+O_3}[OH][O_3] - k_{O(^1D)+H_2O}[O(^1D)][H_2O] - L(O_3 + alkenes) \quad (1)$$

105 where, *k terms* are the reaction rate coefficients; RO_{2i} is the individual organic peroxy radicals.
106 The negative terms in Eq. (1) correspond to the reaction of OH and NO₂ to form nitric acid, the
107 formation of organic nitrates, P(RONO₂), the reactions of OH and HO₂ with O₃, the photolysis of
108 O₃ followed by the reaction of O(¹D) with H₂O, and O₃ reactions with alkenes. Ozone is
109 additionally destroyed by dry deposition.

110 The dependence of O₃ production on NO_x and VOCs can be categorized into two typical
111 scenarios: NO_x sensitive and VOC sensitive. The method proposed by Kleinman [2005b] was
112 used to evaluate the O₃ production sensitivity using the ratio of L_N/Q, where L_N is the radical
113 loss via the reactions with NO_x and Q is the total primary radical production. Because the radical
114 production rate is approximately equal to the radical loss rate, this L_N/Q ratio represents the
115 fraction of radical loss due to NO_x. It was found that when L_N/Q is significantly less than 0.5, the
116 atmosphere is in a NO_x-sensitive regime, and when L_N/Q is significantly greater than 0.5, the
117 atmosphere is in a more VOC-sensitive regime [Kleinman et al., 2001; Kleinman, 2005b]. Note
118 that the contribution of organic nitrates impacts the cut-off value for L_N/Q to determine the ozone
119 production sensitivity to NO_x or VOCs and this value may vary slightly around 0.5 in different
120 environments [Kleinman, 2005b].

121

122

123

124 2.2 Box Model Simulations

125 An observation-constrained box model with the Carbon Bond Mechanism Version 2005
126 (CB05) was used to simulate the oxidation processes in Houston during DISCOVER-AQ.
127 Measurements made on the P-3B were used as input to constrain the box model. From the box
128 model results, the ozone production rate and its sensitivity to NO_x and VOCs were calculated
129 allowing us to calculate ozone production efficiency at different locations and at different times
130 of day.

131 CB05 is a well-known chemical mechanism that has been actively used in research and
132 regulatory applications [Yarwood et al., 2005]. Organic species are lumped according to the
133 carbon bond approach, that is, bond type, e.g., carbon single bond and double bond. Reactions
134 are aggregated based on the similarity of carbon bond structure so that fewer surrogate species
135 are needed in the model. Some organics (e.g., organic nitrates and aromatics) are lumped. The
136 lifetime of alkyl nitrates is too long in CB05 and has been corrected in CB6r2 [Canty et al.,
137 2015], but this should have minimal impact on our findings because the model is constrained to
138 observations as indicated below.

139 The box model was run using measurements, including long-lived inorganic and organic
140 compounds and meteorological parameters (temperature, pressure, humidity, and photolysis
141 frequencies), from the NASA P-3B. One-minute archived data were used as model input
142 (available at <http://www-air.larc.nasa.gov/missions/discover-aq/discover-aq.html>). The model
143 ran for 24 hours for each data point to allow most calculated reactive intermediates to reach
144 steady state, but short enough to prevent the buildup of secondary products. **An additional
145 lifetime of two days was assumed for some calculated long-lived species such as organic acids
146 and alcohols to avoid unexpected accumulation of these species in the model.** At the end of 24
147 hours, the model generated time series of OH, HO₂, RO₂, and other reactive intermediates. The
148 box model covered the entire P-3B flight track during DISCOVER-AQ, including the eight
149 science sites where the P-3B conducted spirals. Note that unlike a three-dimensional chemical
150 transport model, the zero-dimensional box model simulations did not include advection and
151 emissions. Although advection and emissions are certainly important factors for the air pollution
152 formation, they can be omitted in the box model since all of the long-lived radical and O₃
153 precursors were measured and used to constrain the box model calculations. **The box model
154 analysis is necessary for ozone production and its sensitivity to NO_x and VOCs because the box**

155 model was constrained to measured species (e.g., NO, NO₂, CO, HCHO, etc.) and
156 meteorological parameters (e.g., photolysis frequencies) that are essential to calculate ozone
157 production rates. Even though there is good agreement in general between the box model and
158 the 3D model, there are still some differences between the measurements and the output from the
159 3D model that are shown below, e.g., NO_x, CO, HCHO and photolysis frequencies.

160

161 **2.3 WRF-CMAQ Model Simulations**

162 The WRF model was run from 18 August 2013 to 1 October 2013 with nested domains
163 with horizontal resolutions of 36, 12, 4, and 1 km and 45 vertical levels. This work utilized
164 results from the 4 km domain. The modeling domains are shown in Figure 3. WRF was run
165 straight through (i.e., was not re-initialized at all) using an iterative technique developed at the
166 EPA and described in Appel et al. (2014). Observational and analysis nudging were performed
167 on all domains. Model output was saved hourly for the 36 and 12 km domains, every 20 minutes
168 for the 4 km domain, and every 5 minutes for the 1 km domain. WRF and CMAQ configuration
169 options and inputs are shown in Table 1.

170 WRF model results were used to drive the CMAQ model offline. The 2012 baseline
171 anthropogenic emissions from the Texas Commission on Environmental Quality (TCEQ) were
172 used as input to CMAQ. These emissions contain the most-up-to-date Texas anthropogenic
173 emissions inventory and a compilation of emissions estimates from Regional Planning Offices
174 throughout the US. Biogenic emissions were calculated online within CMAQ with Biogenic
175 Emission Inventory System (BEIS). Lightning emissions were also calculated online within
176 CMAQ. CMAQ was run with the process analysis tool to output ozone production rate (P(O₃)),
177 ozone loss rate (L(O₃)), and net ozone production rate (net P(O₃)) as well as ozone production
178 efficiency (OPE).

179

180 **3. RESULTS**

181 **3.1 Photochemical O₃ Production Rate, Sensitivity, and Diurnal Variations**

182 Figure 4 shows the net ozone production rate, net P(O₃), calculated using the box model
183 results along the P-3B flight track for all flight days during the Houston deployment. There are
184 several P(O₃) hotspots over the Houston Ship Channel located to the east/southeast of downtown
185 Houston as well as downwind, over Galveston Bay. This is expected because of large emissions

186 of NO_x and VOCs from the Houston Ship Channel, where the highest $P(\text{O}_3)$ was observed – up
187 to ~ 140 ppbv hr^{-1} . $P(\text{O}_3)$ values up to ~ 80 -90 ppbv hr^{-1} were observed over Galveston Bay,
188 mainly on September 25, 2013, consistent with high ozone levels observed across the Houston
189 area on that day. Similar instantaneous ozone production rates have been observed in two
190 previous studies in Houston in 2000 and 2006 [Kleinman et al., 2002a; Mao et al., 2010].

191 Figure 5 shows the indicator L_N/Q of ozone production sensitivity along the P-3B flight
192 track for all flight days during the Houston deployment. $P(\text{O}_3)$ was mainly VOC-sensitive over
193 the Houston Ship Channel and its surrounding urban areas due to large NO_x emissions. Over
194 areas away from the center of the city with relatively low NO_x emissions, $P(\text{O}_3)$ was usually
195 NO_x -sensitive. Vertical profiles of $P(\text{O}_3)$, $L(\text{O}_3)$, and net ozone production calculated using the
196 box model results (Figure 6) show that:

- 197 (1) $\text{RO}_2 + \text{NO}$ makes about the same amount of O_3 as $\text{HO}_2 + \text{NO}$ in the model;
- 198 (2) O_3 photolysis followed by $\text{O}(^1\text{D}) + \text{H}_2\text{O}$ is a dominant process for the photochemical ozone
199 loss;
- 200 (3) the maximum net $P(\text{O}_3)$ appeared near the surface below 1 km.

201 In the diurnal variations of $P(\text{O}_3)$, a broad peak in the morning with significant $P(\text{O}_3)$ in
202 the afternoon was obtained on ten flight days during DISCOVER-AQ in Houston (Figure 7).
203 High $P(\text{O}_3)$ mainly occurred with $L_N/Q > 0.5$ (i.e., in the VOC sensitive regime). The diurnal
204 variation of L_N/Q indicates that $P(\text{O}_3)$ was mainly VOC sensitive in the early morning and then
205 transitioned towards the NO_x sensitive regime later in the day (Figure 8). High $P(\text{O}_3)$ in the
206 morning was mainly associated with VOC sensitivity due to high NO_x levels in the morning
207 (points in the red circle in Figure 8). Although $P(\text{O}_3)$ was mainly NO_x sensitive in the afternoon
208 between 12:00 and 17:00 Central Standard Time, CST (UTC-6 hours), there were also periods
209 and locations when $P(\text{O}_3)$ was VOC sensitive, e.g., the points with $L_N/Q > 0.5$ between 12:00
210 and 17:00 (CST) in Figure 8.

211 Diurnal variations of ozone production rate at eight individual locations where the P-3B
212 conducted vertical spirals show that the ozone production is greater than 10 ppbv hr^{-1} on average
213 at locations with high NO_x and VOC emissions, such as Deer Park, Moody Tower and
214 Channelview, while at locations away from the urban center with lower emissions, such as
215 Galveston, Smith Point, and Conroe, the ozone production usually averaged less than 10 ppbv hr^{-1}
216 (Figure 9). The dependence of $P(\text{O}_3)$ on the NO mixing ratio ($[\text{NO}]$) shows that when $[\text{NO}]$ is

217 less than ~ 1 ppbv, ozone production increases as the $[\text{NO}]$ increases, i.e., $P(\text{O}_3)$ is in NO_x
218 sensitive regime. When the NO mixing ratio is greater than ~ 1 ppbv, ozone production levels off,
219 i.e., $P(\text{O}_3)$ is in a NO_x saturated regime (Figure 10). It was also found that at a given NO mixing
220 ratio, a higher production rate of HO_x results in a higher ozone production rate. Diurnal
221 variations of the indicator of ozone production sensitivity to NO_x and VOCs, L_N/Q , at eight
222 individual locations where the P-3B conducted vertical spirals show that (1) at Deer Park, $P(\text{O}_3)$
223 was mostly VOC sensitive for the entire day; (2) at Moody Tower and Channelview, $P(\text{O}_3)$ was
224 VOC sensitive or in the transition regime; and (3) at Smith Point and Conroe, $P(\text{O}_3)$ was mostly
225 NO_x sensitive for the entire day; and Galveston, West Houston, and Manvel Croix $P(\text{O}_3)$ was
226 VOC sensitive only in the early morning (Figure 11).

227

228 **3.2 Ozone Production Efficiency**

229 Ozone production efficiency (OPE) is defined as the number of molecules of oxidant O_x
230 ($= \text{O}_3 + \text{NO}_2$) produced photochemically when a molecule of NO_x ($= \text{NO} + \text{NO}_2$) is oxidized. It
231 conveys information about the conditions under which O_3 is formed and is an important
232 parameter to consider when evaluating impacts from NO_x emission sources [Kleinman et al.,
233 2002]. The OPE can be deduced from atmospheric observations as the slope of a graph of O_x
234 concentration versus the concentration of NO_x oxidation products. The latter quantity is denoted
235 as NO_z and is commonly measured as the difference between NO_y (sum of all odd-nitrogen
236 compounds) and NO_x , i.e. $\text{NO}_z = \text{NO}_y - \text{NO}_x$.

237 Figure 12 shows the photochemical oxidant O_x as a function of NO_z during DISCOVER-
238 AQ in Houston in 2013. The two data sets plotted here were collected on September 25 and 26,
239 when high ambient ozone concentrations were observed, and for the data collected during all
240 other flights. Note that the slopes obtained from these two data sets are essentially the same and
241 an average OPE of ~ 8 is derived from the observations, meaning that 8 molecules of ozone were
242 produced when one molecule of NO_x was consumed. Even though higher ozone concentrations
243 were observed on September 25 and 26, the OPE on these two days are not different from those
244 in other flights, indicating the ozone event on these two days was not caused by a higher OPE,
245 but mainly, by higher concentrations of ozone precursors (and thus higher ozone production
246 rates) and background ozone as indicated by the intercepts in the regression of the two data sets
247 in Figure 12. The high ozone observed on those days could also be due to slower ventilation and

248 different meteorological conditions such as a lower boundary layer height, northerly transport
249 from inland air pollution source regions, stagnant conditions from the high-pressure system, and
250 the bay and gulf breezes.

251 The OPE value of ~8 during DISCOVER-AQ in Houston in 2013 is greater than the
252 average OPE value obtained during the Texas Air Quality Study in 2006 (TexAQS2006;
253 OPE=5.9±1.2) [Neuman et al., 2009] and TexAQS2000 (OPE=5.4) [Ryerson et al., 2003]. One
254 possible reason for this increased OPE is the continuous reduction in NO_x emissions in Houston
255 from 2000 to 2013 pushed NO_x levels closer to 1 ppbv in 2013 (Figure S1), thus OPE increased
256 since OPE increases as NO_x decreases when the NO_x level is greater than ~1 ppbv (Figure 13).

257 Houston area OPE values range from about a factor of 1.3 to 2 higher than the OPEs
258 calculated from the DISCOVER-AQ 2011 study in Maryland, likely due to higher
259 photochemical reactivity in Houston (Figure S4). The 2011 Maryland OPEs ranged from 3.4 to
260 6.1 when all measured data below 1 km are used (Ren, X., unpublished data). An OPE of ~8 was
261 calculated [He et al., 2013] for the 2011 Maryland DISCOVER-AQ campaign for measured data
262 below the 850 hPa level during vertical spirals with a strong linear correlation ($r^2 > 0.8$) between
263 O_x and NO_z. Additionally, OPEs of 7.7-9.7 were obtained from a ground site during the New
264 England Air Quality Study (NEAQS) 2002 (Griffin et al., 2004).

265 When calculating ozone production efficiency using observed O_x and NO_z, it is important
266 to know whether there is substantial loss of nitric acid (HNO₃), because it can affect the OPE by
267 reducing the NO_z [Trainer et al., 1993; 2000; Neuman et al., 2009] and thus bias the OPE high.
268 The derived OPE in Figure 12 is only valid when there is minimum loss of NO_z (especially
269 HNO₃) from the source region to the point of observations. Neuman et al. [2009] found that
270 $\Delta\text{CO}/\Delta\text{NO}_y$, i.e., the slope in a CO versus NO_y plot, is an indicator for distinguishing plumes
271 with efficient O₃ formation from plumes with similarly high O₃ to NO_x oxidation products
272 correlation slopes caused by variable mixing of aged polluted air depleted in HNO₃. A typical
273 $\Delta\text{CO}/\Delta\text{NO}_y$ ranges from ~40 in background air to ~4-7 in fresh emission plumes in Houston
274 [Neuman et al., 2009]. The $\Delta\text{CO}/\Delta\text{NO}_y$ was examined at different times of the day on September
275 25 and 26. The results indicate that the $\Delta\text{CO}/\Delta\text{NO}_y$ was about 6.2 (Figure 14a) throughout the
276 day with variation between 6.0 and 7.0 (Figure 14). This demonstrates that the observed O₃
277 formation was from fresh plumes and was not caused by variable mixing of aged polluted air
278 depleted in HNO₃.

279 Using both the box model and CMAQ model results, OPE can also be calculated
280 according to its definition, i.e., the net ozone formation rate divided by the formation rate of
281 NO_z . Net $\text{P}(\text{O}_3)$ was calculated using Eq. (1), while the NO_z formation rate is the sum of HNO_3
282 and organic nitrate formation rates. The agreement between the box model-derived and the
283 CMAQ-derived OPEs is very good, with the mean OPEs of 14.8 ± 7.4 in the box model and
284 16.6 ± 8.1 in the CMAQ model. The dependence of OPE on NO_x is also similar for both the box
285 and CMAQ models (Figure 13). On average, the maximum of OPE appears at a NO_x level
286 around 1 ppbv. In general, if the NO_x level is below 1 ppbv, OPE increases as the NO_x level
287 increases, while if the NO_x level is above 1 ppbv, OPE decreases as the NO_x level increases
288 (Figure 13).

289 The OPE values calculated using the CMAQ and box model are greater than the values
290 derived from the observations using the slope in the scatter plot of Ox versus NO_z in Figure 12.
291 This is expected because in the calculation of OPE using the box and CMAQ model results, a
292 few ozone loss processes, such as ozone dry deposition and horizontal/vertical dispersion, were
293 not considered. This could result in higher calculated ozone production rates using the model
294 results.

295 Spatial variations of OPE demonstrate that except for a few hotspots over Downtown
296 Houston and the Houston Ship Channel, most large OPEs appear away from the urban center,
297 e.g., the northwest and southeast of the area, while in areas with high NO_x emissions close to the
298 urban center lower OPEs were generally observed (Figure 15). This is again consistent with the
299 results in Figure 13 that the maximum of OPE appears at a NO_x level around 1 ppbv.

300

301 **4. Discussion and Conclusions**

302 On average, ozone production $\text{P}(\text{O}_3)$, was about 20-30 ppbv hr^{-1} in the morning and 5-10
303 ppbv hr^{-1} in the afternoon during DISCOVER-AQ in Houston in 2013. The diurnal variation of
304 $\text{P}(\text{O}_3)$ shows a broad peak in the morning with significant $\text{P}(\text{O}_3)$ in the afternoon obtained on ten
305 flight days in September 2013. High $\text{P}(\text{O}_3)$ mainly occurred with L_N/Q greater than 0.5, i.e., in
306 the VOC sensitive regime. Since $\text{P}(\text{O}_3)$ depends on NO_x levels and radical production rate, it
307 increases as $[\text{NO}]$ increases up to ~ 1 ppbv and then levels off with further increases of $[\text{NO}]$. At
308 a given $[\text{NO}]$, a higher production rate of HO_x results in a higher ozone production rate. This has
309 implications for the NO_x control strategies in order to achieve the ozone control goal.

310 The DISCOVER-AQ campaign in Houston is unique because of its large spatial coverage
311 and thus spatial variations of ozone production and its sensitivity to NO_x and VOCs. Diurnal
312 variations of P(O₃) at eight individual locations where the P-3B conducted vertical spirals show
313 that the P(O₃) is on average more than 10 ppbv hr⁻¹ at locations with high NO_x and VOC
314 emissions, such as Deer Park, Moody Tower, and Channelview, while at locations away from the
315 urban center with lower emissions of ozone precursors such as Galveston, Smith Point, and
316 Conroe, the ozone production rate is usually less than 10 ppbv hr⁻¹ on average. Hotspots of P(O₃)
317 were observed over Downtown Houston and the Houston Ship Channel due to significant
318 emissions in these areas.

319 Ozone production tended more towards VOC sensitive in the morning with high P(O₃)
320 and in general, NO_x sensitive in the afternoon with some exceptions. It was found that during
321 some afternoon time periods and locations, P(O₃) was VOC sensitive. The diurnal variation of
322 L_N/Q indicates that P(O₃) was mainly VOC sensitive in the early morning and then transitioned
323 towards the NO_x sensitive regime later in the day. High P(O₃) in the morning was mainly
324 associated with VOC sensitivity due to high NO_x levels in the morning. Specifically, Deer Park
325 was mostly VOC sensitive for the entire day, Moody Tower and Channelview were VOC
326 sensitive or in the transition regime, and Smith Point and Conroe were mostly NO_x sensitive for
327 the entire day.

328 Based on the measurements on the P-3B, ozone production efficiency (OPE) was about 8
329 during DISCOVER-AQ 2013 in Houston. This OPE value is greater than the average OPE value
330 (5.9±1.2) obtained during the Texas Air Quality Study in 2006 (TexAQS2006), likely due to the
331 reduction in NO_x emissions in Houston between 2006 and 2013 that pushed NO_x levels closer to
332 1 ppbv in 2013 from higher NO_x levels in previous years. The results from this work strengthen
333 our understanding of O₃ production; they indicate that controlling NO_x emissions will provide air
334 quality benefits over the greater Houston metropolitan area in the long run, but in selected areas
335 controlling VOC emissions will also be beneficial.

336

337 **Acknowledgements**

338 The authors acknowledge the entire DISCOVER-AQ science team for the use of the P-
339 3B measurement data in this work as well as Winston Luke and Paul Kelley at NOAA Air
340 Resources Laboratory for helpful discussion. This work was funded by the Texas Commission

341 on Environmental Quality (TCEQ) through the Air Quality Research Program (AQRP) at
342 University of Texas Austin (Contract #14-020). The contents, findings, opinions, and
343 conclusions are the work of the authors and do not necessarily represent the findings, opinions,
344 or conclusions of the TCEQ or AQRP. NASA AQUEST supported RRD.

345

346

347 **References**

348 Appel, K.W., Gilliam, R.C., Pleim, J.E., Pouliot, G.A., Wong, D.C., Hogrefe, C., Roselle, S.J.,
349 and Mathur, R.: Improvements to the WRF-CMAQ modeling system for fine-scale air
350 quality simulations, EM, 16-21 2014.

351 Canty, T. P., Hemberck, L., Vinciguerra, T. P. , Anderson, D. C. , Goldberg, D. L. , Carpenter, S.
352 F. , Allen, D. J. , Loughner, C. P. , Salawitch, R. J. , and Dickerson, R. R.: Ozone and NOx
353 chemistry in the eastern US: evaluation of CMAQ/CB05 with satellite (OMI) data,
354 *Atmospheric Chemistry and Physics*, 15(19), 10965-10982, doi:10.5194/acp-15-10965-2015,
355 2015.

356 Chen, S., Ren, X., Mao J., Chen, Z., Brune, W. H., Lefer, B., Rappenglück, B., Flynn J., Olson,
357 J., Crawford, J. H.: A comparison of chemical mechanisms based on TRAMP–2006 field
358 data, *Atmos. Environ.*, 44(33), 4116-4125, 2010.

359 DISCOVER-AQ whitepaper, [http://discover-aq.larc.nasa.gov/pdf/DISCOVER-](http://discover-aq.larc.nasa.gov/pdf/DISCOVER-AQ_science.pdf)
360 [AQ_science.pdf](http://discover-aq.larc.nasa.gov/pdf/DISCOVER-AQ_science.pdf).

361 Finlayson-Pitts, B. J., and Pitts, J.: Chemistry of the upper and lower atmosphere: Theory,
362 experiments and applications, Academic Press, San Diego, California, p.264-276, 2000.

363 Goldberg, D. L., Vinciguerra, T. P., Anderson, D. C., Hemberck, L., Canty, T. P., Salawitch, R.
364 J., and Dickerson, R. R. CAMx Ozone Source Attribution in the Eastern United States using
365 Guidance from Observations during DISCOVER-AQ Maryland, *Geophysical Research*
366 *Letters*, doi: 10.1002/2015GL067332, 2016.

367

368 Griffin, R. J., Johnson, C. A., Talbot, R. W., Mao, H., Russo, R. S., Zhou, Y., and Sive B. C.:
369 Quantification of ozoneformation metrics at Thompson Farm during the New England Air
370 Quality Study (NEAQS) 2002, *J. Geophys. Res.*, 109, D24302,doi:10.1029/2004JD005344,
371 2004.

372 He, H., Hemberck, L., Hosley, K. M., Canty, T. P., Salawitch, R. J., and Dickerson, R. R.: High
373 ozone concentrations on hot days: The role of electric power demand and NO_x emissions,
374 *Geophys. Res. Lett.*, 40, 5291–5294, doi:[10.1002/grl.50967](https://doi.org/10.1002/grl.50967), 2013.

375

376 Jacob, D. J.: *Introduction to Atmospheric Chemistry*, Princeton University Press, New Jersey,
377 1999.

378 Kleinman, L. I., Daum, P. H., Lee, Y.-N., Nunnermacker, L. J., Springston, S. R., Weinstein-
379 Lloyd J., and Rudolph, J.: Sensitivity of ozone production rate to ozone precursors. *Geophys.*
380 *Res. Lett.*, 28, 2903–2906, doi: [10.1029/2000GL012597](https://doi.org/10.1029/2000GL012597), 2001.

381 Kleinman, L. I., Daum, P. H., Lee, Y.-N., Nunnermacker, L. J., Springston, S. R., Weinstein-
382 Lloyd, J., and Rudolph, J.: Ozone production efficiency in an urban area, *J. Geophys. Res.*,
383 107 (D23), 4733, doi:[10.1029/2002JD002529](https://doi.org/10.1029/2002JD002529), 2002.

384 Kleinman, L. I., Daum, P. H., Lee, Y.-N., Nunnermacker, L. J., Springston, S. R., Weinstein-
385 Lloyd, J., and Rudolph, J.: A comparative study of ozone production in five U.S.
386 metropolitan areas, *J. Geophys. Res.*, 110, D02301, doi:[10.1029/2004JD005096](https://doi.org/10.1029/2004JD005096), 2005a.

387 Kleinman, L. I.: The dependence of tropospheric ozone production rate on ozone precursors,
388 *Atmos. Environ.*, 39(3), 575–586, doi:[10.1016/j.atmosenv.2004.08.047](https://doi.org/10.1016/j.atmosenv.2004.08.047), 2005b.

389 Lei, W., Zhang, R., Tie, X., and Hess, P.: Chemical characterization of ozone formation in the
390 Houston-Galveston area: A chemical transport model study, *J. Geophys. Res.*, 109, D12301,
391 doi:[10.1029/2003JD004219](https://doi.org/10.1029/2003JD004219), 2004.

392 Li, G., Zhang, R., Fan, J., and Tie, X.: Impacts of biogenic emissions on photochemical ozone
393 production in Houston, Texas, *J. Geophys. Res.*, 112, D10309, doi:[10.1029/2006JD007924](https://doi.org/10.1029/2006JD007924),
394 2007.

395 Mallet, V. and Sportisse, B.: A comprehensive study of ozone sensitivity with respect to
396 emissions over Europe with a chemistry-transport model, *J. Geophys. Res.*, 110, D22302,
397 doi:[10.1029/2005JD006234](https://doi.org/10.1029/2005JD006234), 2005.

398 Mao, J., Ren, X., Chen, S., Brune, W. H., Chen, Z., Martinez, M., Harder, H., Lefer, B.,
399 Rappenglück, B., Flynn, J., and Leuchner, M.: Atmospheric oxidation capacity in the
400 summer of Houston 2006: Comparison with summer measurements in other metropolitan
401 studies, *Atmos. Environ.*, 44(33), 4107-4115, 2010

402 Molina, M. J., and Molina, L. T.: Megacities and atmospheric pollution, *J. Air Waste Manage.*,

403 54, 644–680, 2004.

404 Neuman, J. A., et al.: Relationship between photochemical ozone production and NO_x oxidation
405 in Houston, Texas, *J. Geophys. Res.*, 114, D00F08, doi:10.1029/2008JD011688, 2009.

406 Ren, X., van Duin, D., Cazorla, M., Chen, S., Mao, J., Zhang, L., Brune, W. H., Flynn, J. H.,
407 Grossberg, N., Lefer, B. L., Rappenglück, B., Wong, K. W., Tsai, C., Stutz, J., Dibb, J. E.,
408 Jobson, B. T., Luke, W. T., and Kelley, P.: Atmospheric oxidation chemistry and ozone
409 production: Results from SHARP 2009 in Houston, Texas, *J. Geophys. Res.*, 118, 5770–
410 5780, 2013.

411 Ryerson, T. B., et al., Effect of petrochemical industrial emissions of reactive alkenes and NO_x
412 on tropospheric ozoneformation in Houston, Texas, *J. Geophys. Res.*, 108(D8), 4249,
413 doi:10.1029/2002JD003070, 2003.

414 Sillman, S.: The use of NO_y, H₂O₂, and HNO₃ as indicators for O₃-NO_x-hydrocarbon sensitivity
415 in urban locations, *J. Geophys. Res.*, 100, 14,175–14,188, 1995.

416 Sillman, S., Vautard, R., Menut, L., and Kley, D.: O₃-NO_x-VOC sensitivity and NO_x-VOC
417 indicators in Paris: Results from models and Atmospheric Pollution Over the Paris Area
418 (ESQUIF) measurements, *J. Geophys. Res.*, 108(D17), 8563, doi:10.1029/2002JD001561,
419 2003.

420 Tang, X., Wang, Z., Zhu, J., Gbaguidi, A. E., Wu, Q., Li, J., and Zhu, T., Sensitivity of ozone to
421 precursor emissions in urban Beijing with a Monte Carlo scheme. *Atmos. Environ.*, 44, 3833-
422 3842, 2010.

423 Thielmann, A., Prevo^ot, A. S. H., and Staehelin, J.: Sensitivity of ozone production derived
424 from field measurements in theItalian Po basin, *J. Geophys. Res.*, 107(D22), 8194,
425 doi:10.1029/2000JD000119, 2002.

426 Trainer, M., et al.: Correlation of ozone with NO_y in photochemically aged air, *J. Geophys. Res.*,
427 98, 2917 – 2925, doi:10.1029/ 92JD01910, 1993.

428 Trainer, M., Parrish, D. D., Goldan, P. D., Roberts, J., and Fehsenfeld, F. C.: Review of
429 observation-based analysis of the regional factors influencing ozone concentrations, *Atmos.*
430 *Environ.*, 34, 2045 – 2061, doi:10.1016/S1352-2310(99)00459-8, 2000.

431 Xue, L. K., Wang, T., Gao, J., Ding, A. J., Zhou, X. H., Blake, D. R., Wang, X. F., Saunders, S.
432 M., Fan, S. J., Zuo, H. C., Zhang, Q. Z., and Wang, W. X.: Ozone production in four major
433 cities of China: sensitivity to ozone precursors and heterogeneous processes, *Atmos. Chem.*

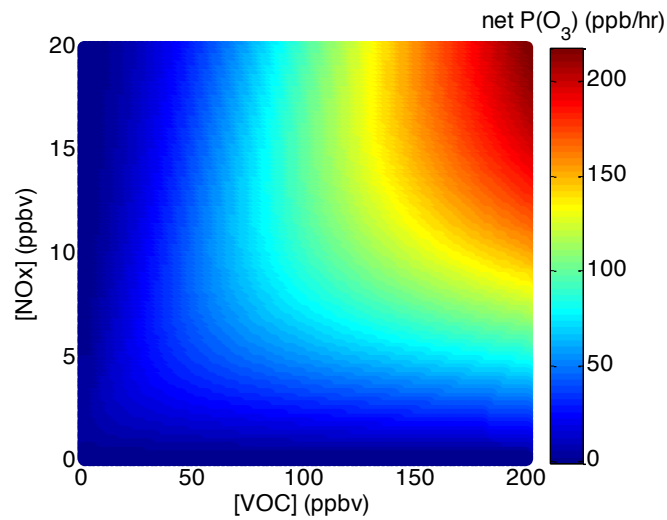
434 Phys. Discuss., 13, 27,243–27,285, doi:10.5194/acpd-13-27243-2013, 2013.
435 Yarwood, G., Rao, S., Yocke, M., and Whitten, G. Z.: Updates to the Carbon Bond Mechanism:
436 CB05, Final Report to the US EPA (RT-0400675),([http://www.camx.com/publ/
437 pdfs/CB05_Final_Report_120805.pdf](http://www.camx.com/publ/pdfs/CB05_Final_Report_120805.pdf)), 2005.
438 Zaveri, R. A., Berkowitz, C. M., Kleinman, L. I., Springston, S. R., Doskey, P. V., Lonneman,
439 W. A., and Spicer, C. W.: Ozone production efficiency and NO_x depletion in an urban
440 plume: Interpretation of field observations and implications for evaluating O₃-NO_x-VOC
441 sensitivity, J. Geophys. Res., 108(D14), 4436, doi:10.1029/2002JD003144, 2003.
442

443 **Table 1.** WRF and CMAQ model options that were used in both the original and improved
 444 modeling scenarios.

Weather Research and Forecasting (WRF) Version 3.6.1 Model Options	
Radiation	Long Wave: Rapid Radiative Transfer Model (RRTM) Short Wave: Goddard
Surface Layer	Pleim-Xiu
Land Surface Model	Pleim-Xiu
Boundary Layer	Asymmetric Convective Model (ACM2)
Cumulus	Kain-Fritsch
Microphysics	WRF Single-Moment 6 (WSM-6)
Nudging	Observational and analysis nudging
Damping	Vertical velocity and gravity waves damped at top of modeling domain
SSTs	Multi-scale Ultra-high Resolution (MUR) SST analysis (~1 km resolution)
Meteorological Initial and Boundary Conditions and Analysis Nudging Inputs	NAM 12 km
Observational Nudging Inputs	NCEP ADP Global Surface and Upper Air Observational Weather Data
CMAQ Version 5.0.2 Model Options	
Chemical Mechanism	Carbon Bond (CB05)
Aerosol Module	Aerosols with aqueous extensions version 5 (AE5)
Dry deposition	M3DRY
Vertical diffusion	Asymmetric Convective Model 2 (ACM2)
Emissions	2012 TCEQ anthropogenic emissions Biogenic Emission Inventory System (BEIS) calculated within CMAQ
Chemical Initial and Boundary Conditions	Model for OZone and Related chemical Tracers (MOZART) Chemical Transport Model (CTM)

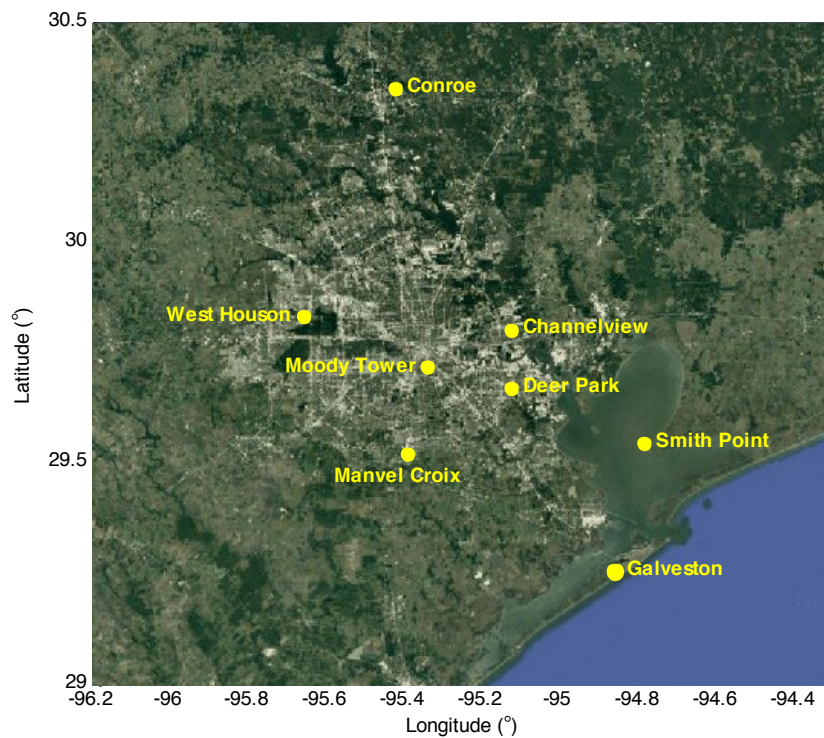
445
 446
 447
 448
 449
 450
 451
 452
 453
 454
 455
 456

457 **Figures:**



458

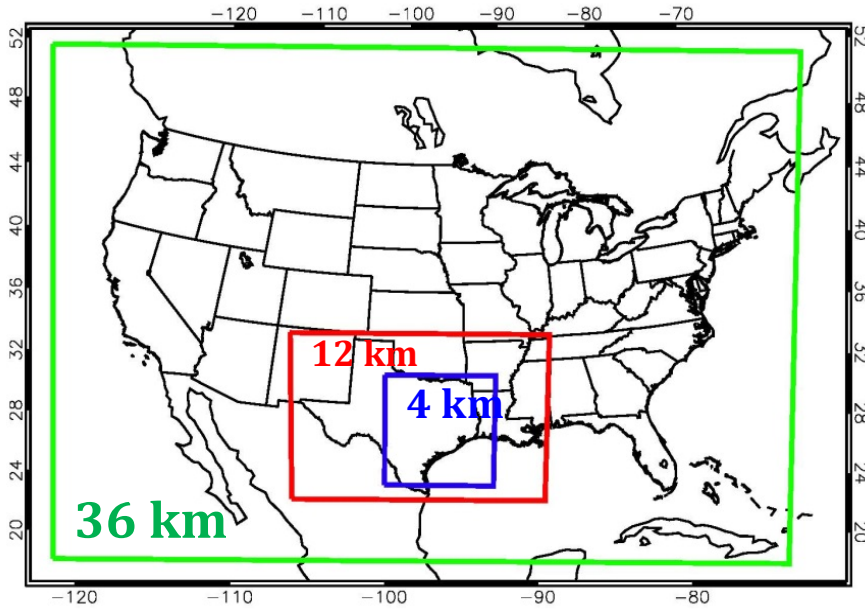
459 **Figure 1.** Ozone production empirical kinetic modeling approach (EKMA) diagram using a box
460 model results with NO_x levels varying from 0-20 ppbv and VOC levels from 0-200 ppbv while
461 the mean concentrations of other species and the speciation of NO_x and VOCs observed during
462 DISCOVER-AQ in Houston in 2013 were used to constrain the box model. This diagram clearly
463 shows the sensitivity of ozone production to NO_x and VOCs in Houston.



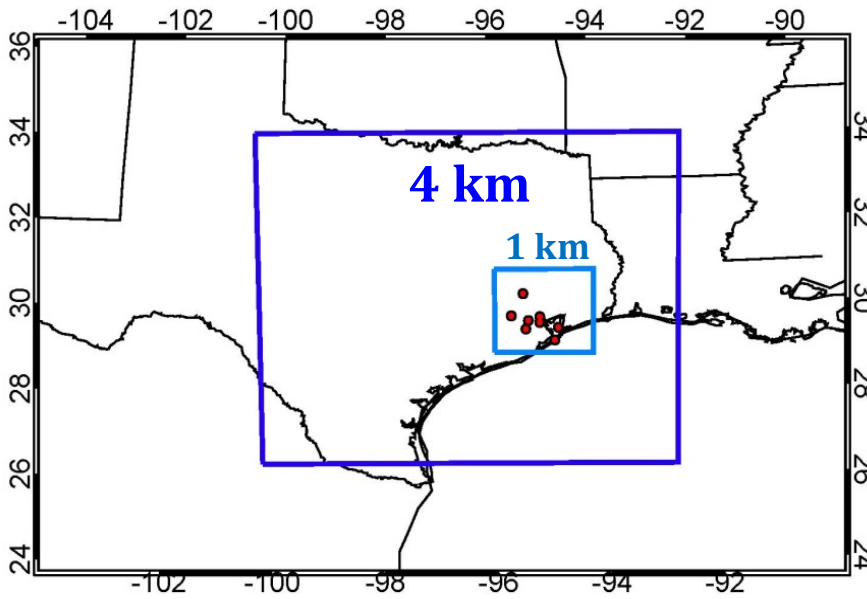
464

465
466
467
468

Figure 2. DISCOVER-AQ ground and spiral sites (yellow dots) during the September 2013 Houston campaign.



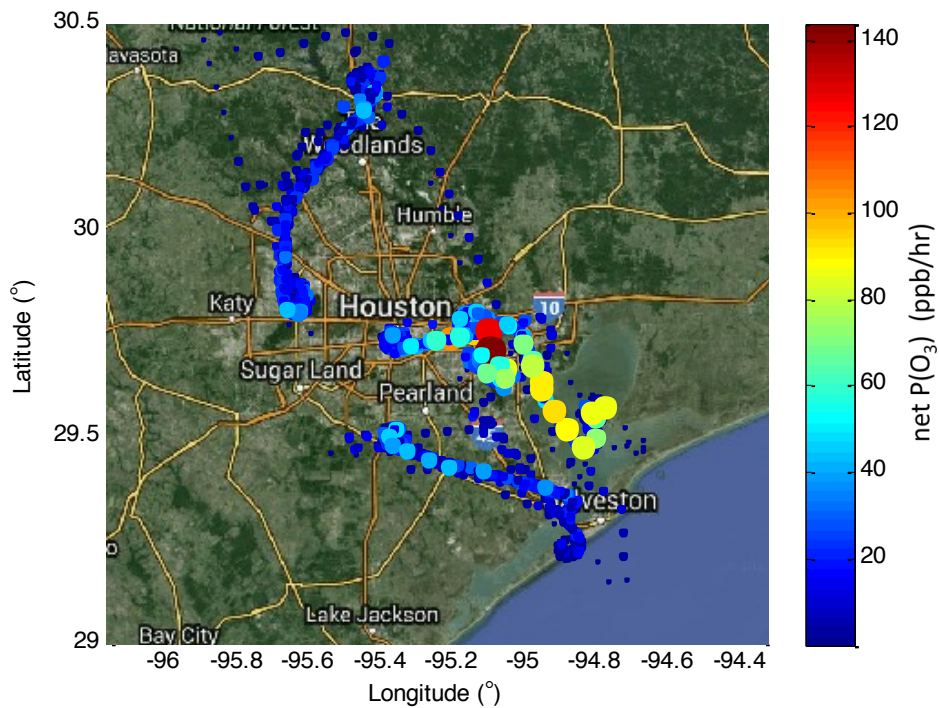
469



470
471
472
473

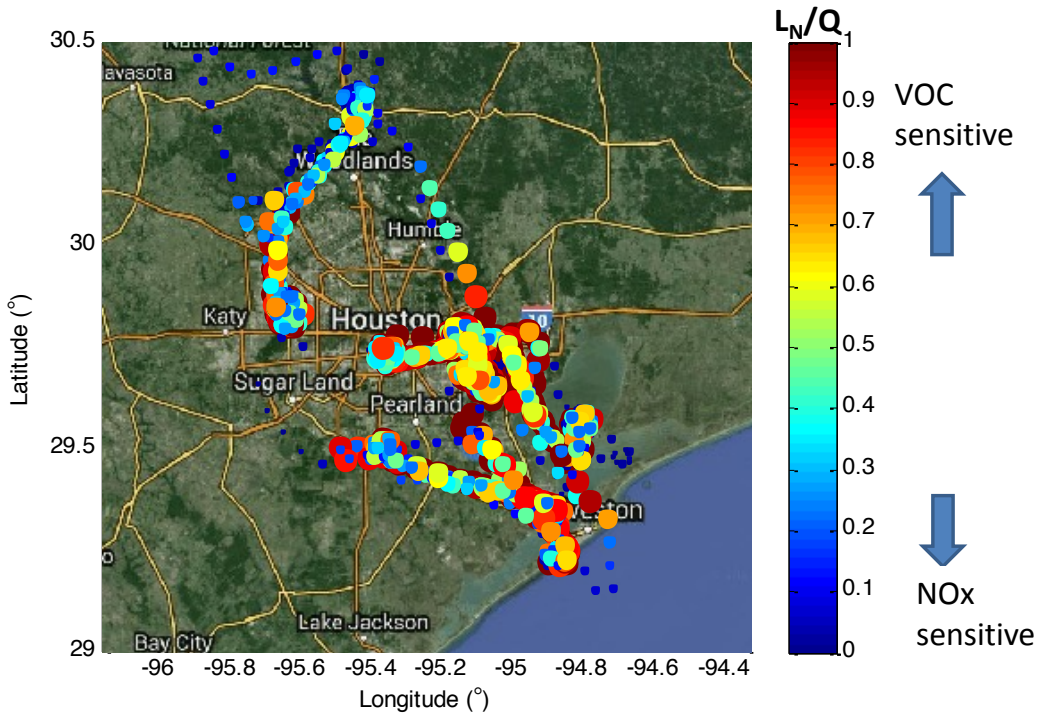
Figure 3. 36, 12, and 4 km CMAQ modeling domains (top); 4 and 1 km CMAQ modeling domains. The red dots show the NASA P-3B aircraft spiral locations (bottom).

474
475
476



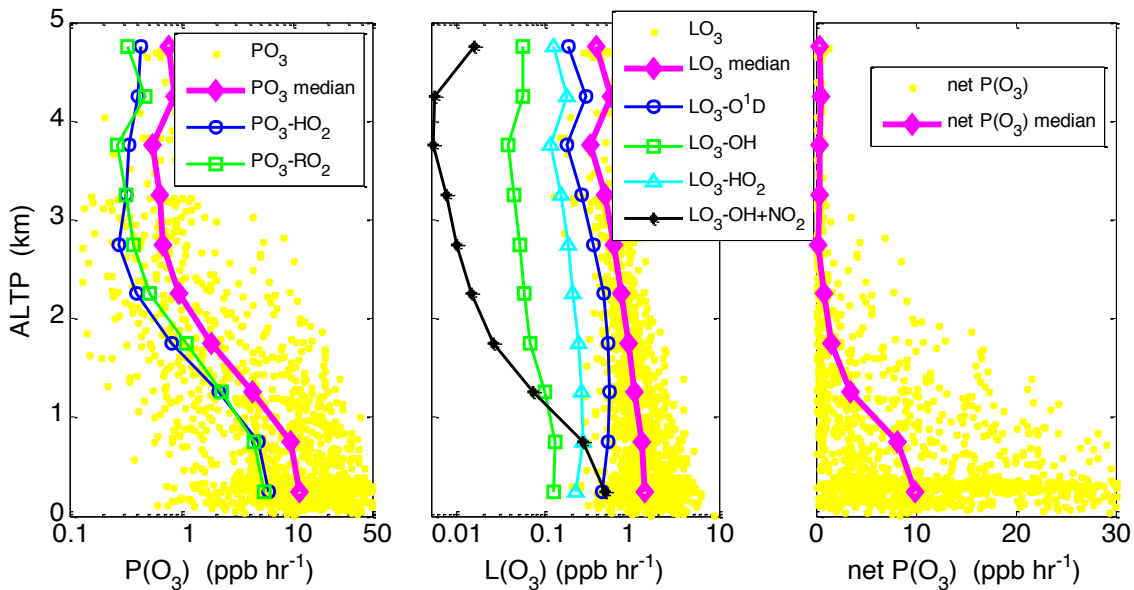
477

478 **Figure 4.** Net ozone production rate, net P(O₃) calculated using the box model results along the
479 P-3B flight track during DISCOVER-AQ in Houston in 2013. The size of dots is proportional to
480 P(O₃).



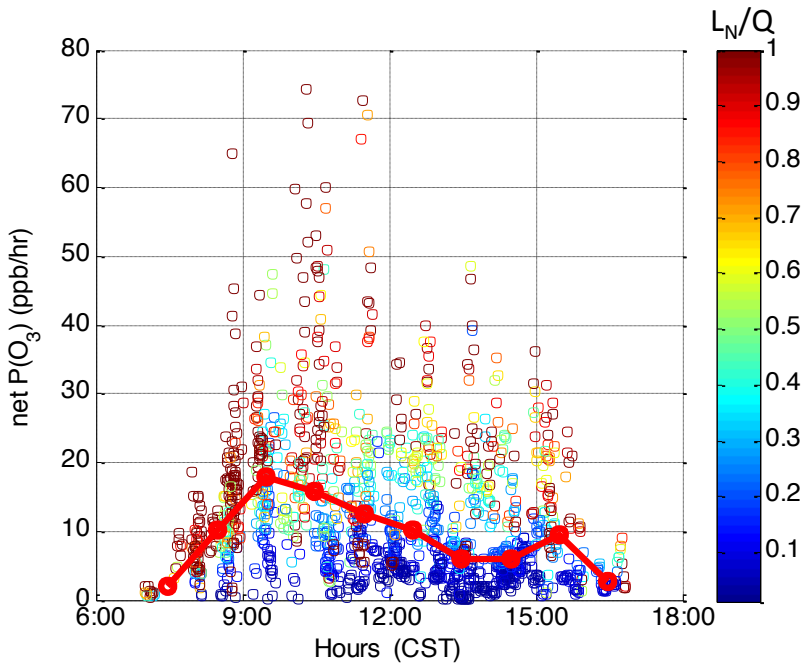
481

482 **Figure 5.** Ozone production sensitivity indicator, L_N/Q , along the P-3B flight track during
 483 DISCOVER-AQ in Houston in 2013. $P(O_3)$ is VOC-sensitive when $L_N/Q > 0.5$, and NOx-
 484 sensitive when $L_N/Q < 0.5$.



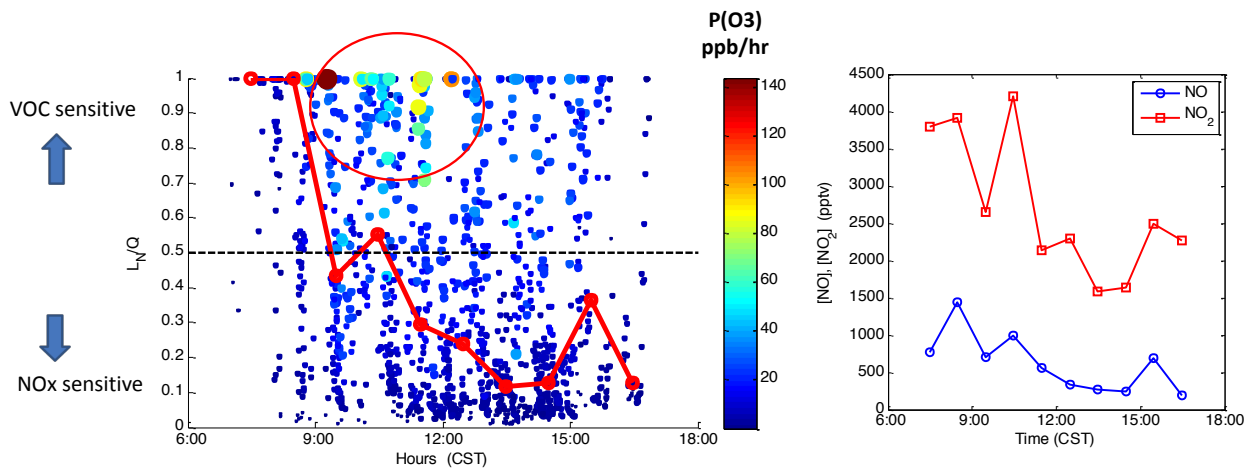
485

486 **Figure 6.** Vertical profiles of ozone production rate (left), ozone loss rate (middle), and net
 487 ozone production rate (right) during DISCOVER-AQ in Houston in 2013.



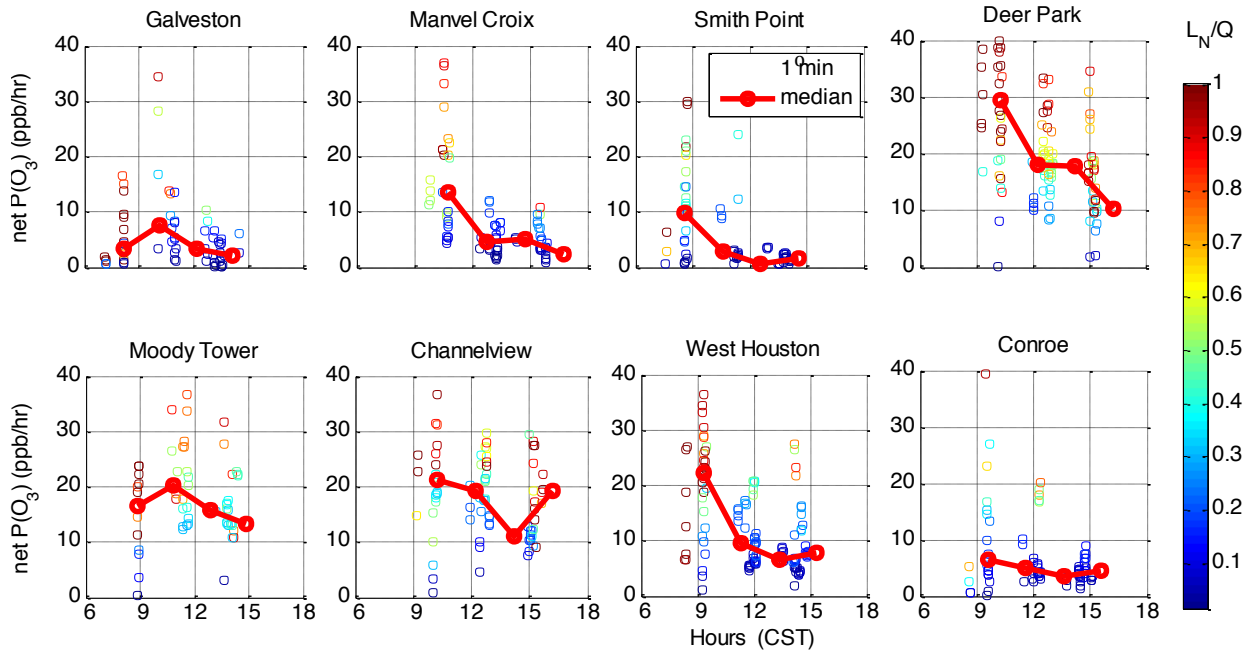
488

489 **Figure 7.** Diurnal variation of ozone production rate colored with the indicator L_N/Q on ten
 490 flight days during DISCOVER-AQ in Houston in 2013. The solid red circles represent the
 491 median values in hourly bins of $P(O_3)$. Data are limited with the pressure altitude less than 1000
 492 m to represent the lowest layer of the atmosphere.



493

494 **Figure 8.** Diurnal variations of the indicator L_N/Q of ozone production rate sensitivity colored
 495 with ozone production rate and median hourly bins of L_N/Q shown in solid red circles (left) and
 496 median hourly NO and NO₂ concentrations (right) below 1000 m during DISCOVER-AQ in
 497 Houston in 2013.

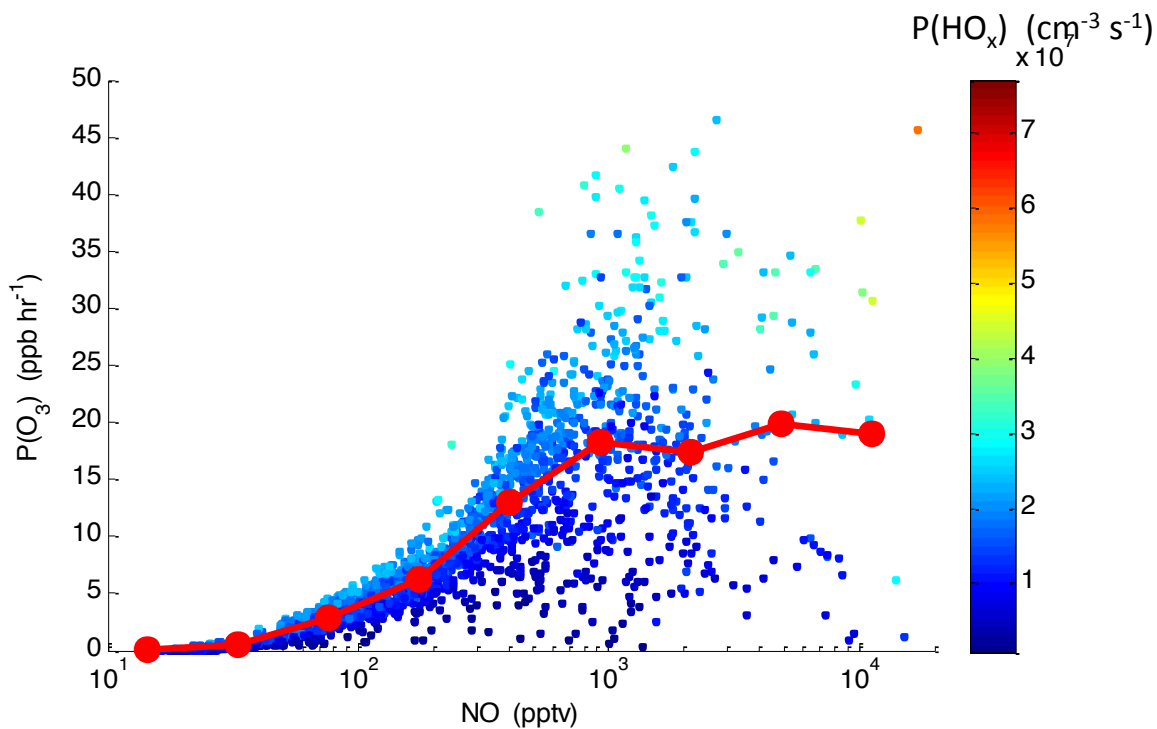


498

499 **Figure 9.** Diurnal variations of ozone production rate at eight individual spiral locations.
 500 Individual points are 1-min data colored with L_N/Q and the linked red circles represent the
 501 median values in hourly bins of $P(O_3)$. Data are limited with the pressure altitude less than 1000
 502 m to represent the lowest layer of the atmosphere.

503

504

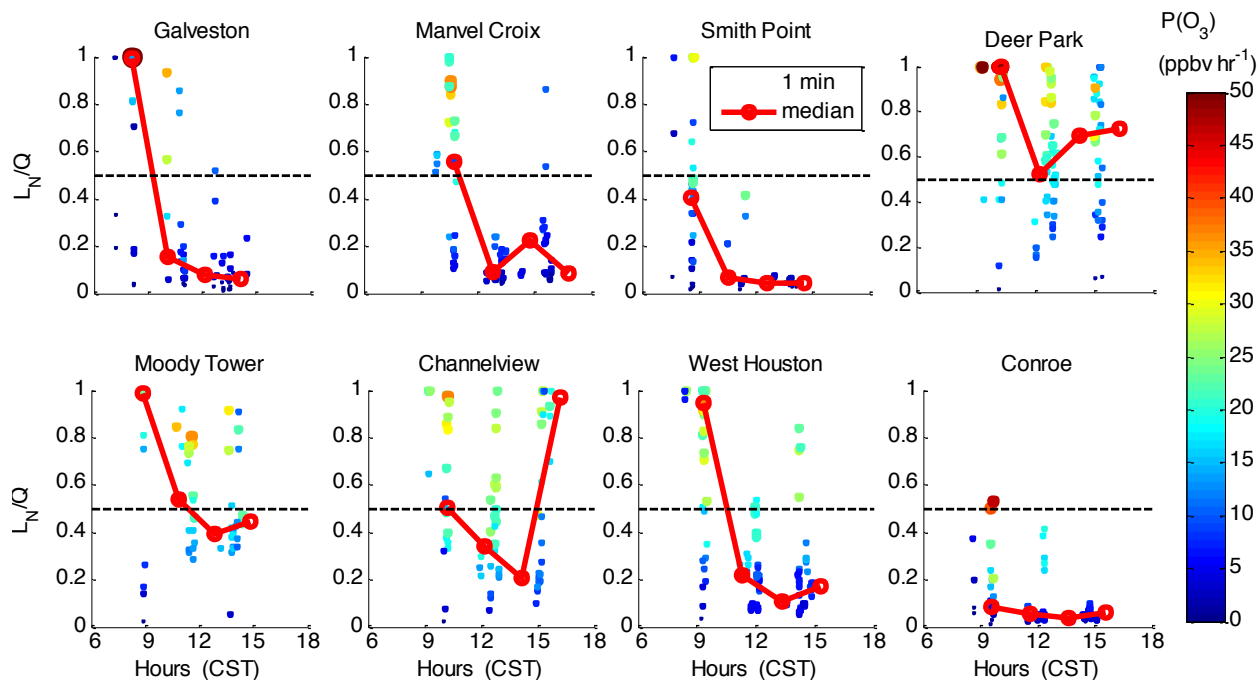


505

506 **Figure 10.** Ozone production as a function of NO mixing ratio. Individual data points are the 1-
 507 minute averages and are colored with the production rate of HO_x (= OH + HO₂) during
 508 DISCOVER-AQ in Houston in 2013. The linked solid red circles represent the median values in
 509 [NO] bins. Note a log scale is used for the x-axis.

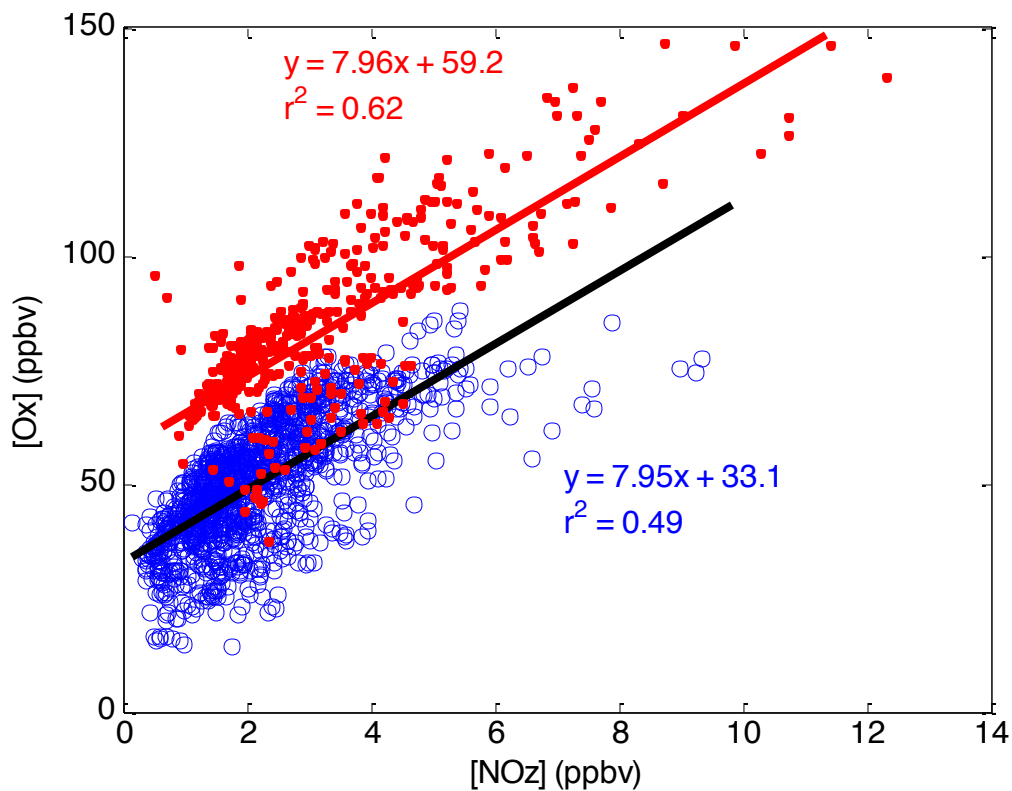
510

511



512

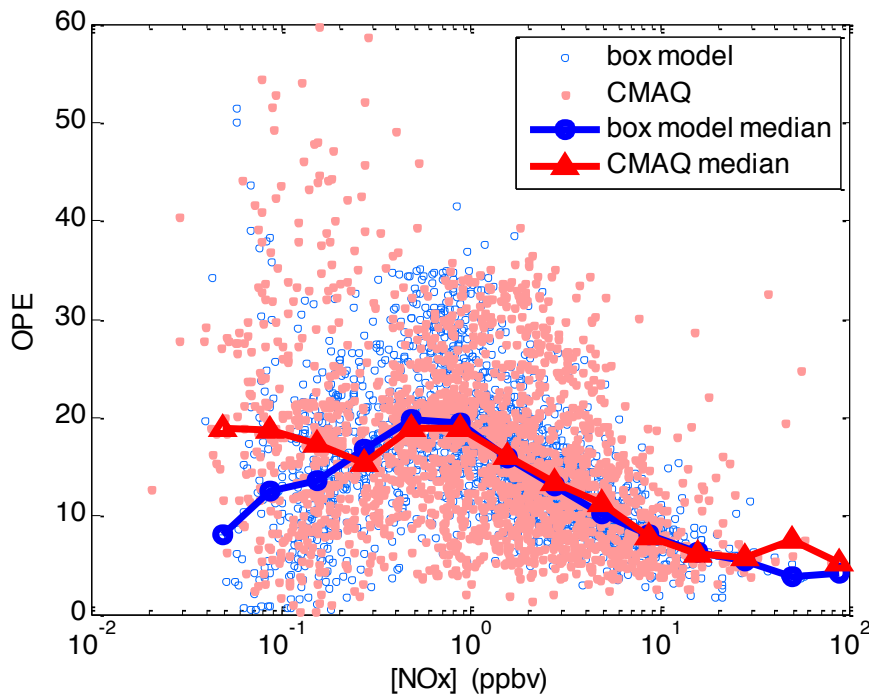
513 **Figure 11.** Diurnal variations of the indicator of ozone production sensitivity to NO_x and VOCs,
 514 L_N/Q , at eight individual spiral locations during DISCOVER-AQ in Houston in 2013. Individual
 515 points are 1-min data colored by $P(O_3)$ and the linked red circles represent the median values in
 516 hourly bins of $P(O_3)$. Data are limited with the pressure altitude less than 1000 m to represent the
 517 lowest layer of the atmosphere.



518

519 **Figure 12.** Photochemical oxidant, Ox (=O₃+NO₂) as a function of NOz (=NO_y-NO_x) during
 520 DISCOVER-AQ in Houston in 2013. Red dots are the data collected on September 25 and 26,
 521 2013 when high ambient ozone concentrations were observed. Blue circles are the data collected
 522 during other flights. Data are limited with the pressure altitude less than 1000 m to represent the
 523 lowest layer of the atmosphere.

524
 525
 526
 527
 528



529

530 **Figure 13.** Ozone production efficiency (OPE) versus NO_x in the box model (blue circles) and
 531 CMAQ model (pink dots) results. The linked blue circles show the median OPE values binned
 532 by NO_x concentration in the box model, while the linked red triangles show the median OPE
 533 values binned by NO_x concentration in the CMAQ model, OPE is calculated according to its
 534 definition as the net ozone formation rate divided by of the formation rate of NO_z.

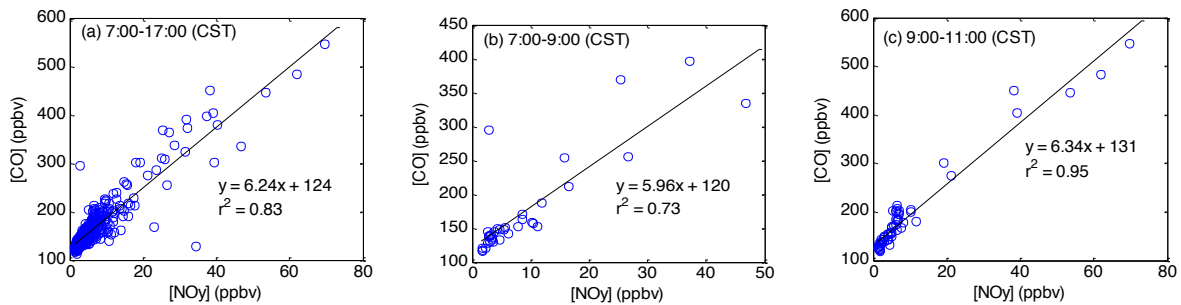
535

536

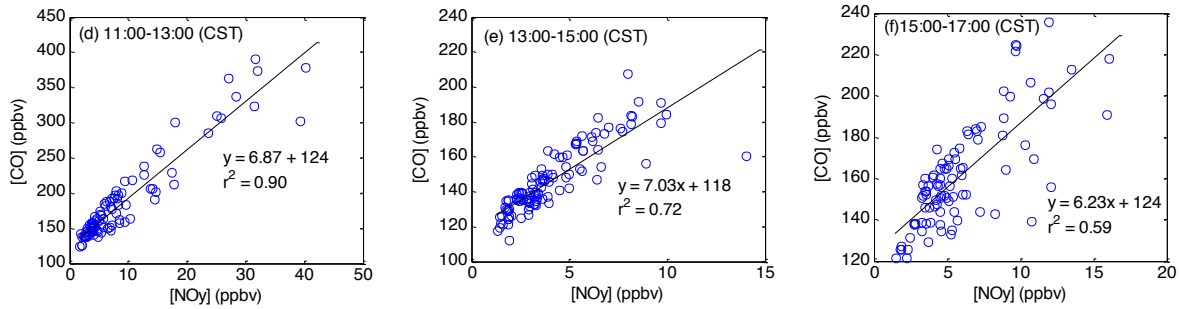
537

538

539

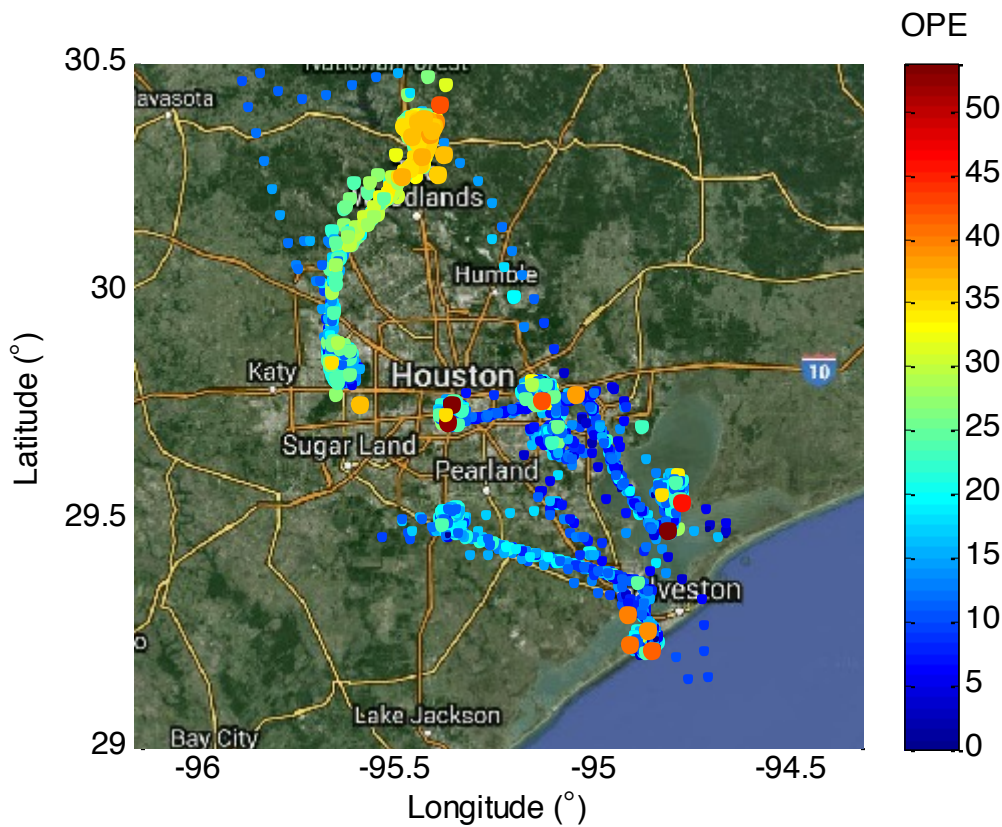


540



541
542
543
544
545

Figure 14. CO versus NO_y and linear regression on September 25 and 26 at different times of the day: (a) 07:00-17:00 (all data), (b) 07:00-09:00, (c) 09:00-11:00, (d) 11:00-13:00, (e) 13:00-15:00, and (f) 15:00-17:00 (CST).



546
547
548
549
550

Figure 15. Ozone production efficiency (OPE) along the P-3B flight track during DISCOVER-AQ in Houston in 2013. OPE was calculated using the box model results as the ratio of net ozone formation rate to the formation rate of NO_z.

